Nucleic Acids Research, 2024, **52**, 4198–4214
https://doi.org/10.1093/nar/gkae084
Advance access publication date: 5 March 2024
Gene regulation, Chromatin and Epigenetics

Set2 regulates Ccp1 and Swc2 to ensure centromeric stability by retargeting CENP-A

Kim Kiat Lim[1,†], Ulysses Tsz Fung Lam[1,†], Ying Li[2,3], Yi Bing Zeng[1], Henry Yang[2,3,4] and Ee Sin Chen[1,2,4,5,*]

[1]Department of Biochemistry, Yong Loo Lin School of Medicine, National University of Singapore, Singapore
[2]NUS Center for Cancer Research, Yong Loo Lin School of Medicine, National University of Singapore, Singapore
[3]Cancer Science Institute, Yong Loo Lin School of Medicine, National University of Singapore, Singapore
[4]National University Health System, Singapore
[5]Integrative Sciences & Engineering Programme, National University of Singapore, Singapore

[*]To whom correspondence should be addressed. Tel: +65 6516 5616; Email: bchces@nus.edu.sg
[†]The first two authors should be regarded as Joint First Authors.

Abstract

Precise positioning of the histone-H3 variant, CENP-A, ensures centromere stability and faithful chromosomal segregation. Mislocalization of CENP-A to extra-centromeric loci results in aneuploidy and compromised cell viability associated with formation of ectopic kinetochores. The mechanism that retargets mislocalized CENP-A back to the centromere is unclarified. We show here that the downregulation of the histone H3 lysine 36 (H3K36) methyltransferase Set2 can preserve centromere localization of a temperature-sensitive mutant *cnp1-1 Schizosaccharomyces pombe* CENP-A (SpCENP-A) protein and reverse aneuploidy by redirecting mislocalized SpCENP-A back to centromere from ribosomal DNA (rDNA) loci, which serves as a sink for the delocalized SpCENP-A. Downregulation of *set2* augments Swc2 (SWR1 complex DNA-binding module) expression and releases histone chaperone Ccp1 from the centromeric reservoir. Swc2 and Ccp1 are directed to the rDNA locus to excavate the SpCENP-A$^{cnp1\text{-}1}$, which is relocalized to the centromere in a manner dependent on canonical SpCENP-A loaders, including Mis16, Mis17 and Mis18, thereby conferring cell survival and safeguarding chromosome segregation fidelity. Chromosome missegregation is a severe genetic instability event that compromises cell viability. This mechanism thus promotes CENP-A presence at the centromere to maintain genomic stability.

Graphical abstract

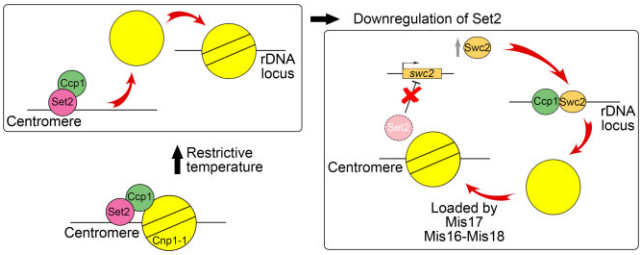

Introduction

Genomic integrity is essential for the precise inheritance of genetic and epigenetic information. Proper segregation of replicated chromosomes during the mitotic phase of cell division preserves genomic integrity, and loss of fidelity of this partitioning process results in aneuploidy, with progeny cells hosting unequal chromosomes (1,2). Aneuploidy represents a major form of genomic instability that can lead to gross deregulation of gene expression and cell death, and is commonly associated with developmental defects and cancer in humans (2–4).

The centromere is the chromosomal locus essential for ensuring proper chromosome segregation. It specifies the site for the assembly of the multi-protein kinetochore complex to enable the capture of spindle microtubules onto the chromosome during mitosis (5). DNA sequences and lengths of the centromeres vary greatly among different organisms ranging from the ∼100 base pairs 'point' centromere in budding yeasts to 'regional' centromeres that stretch for a few kilo- to mega-base pairs in other eukaryotes, including fission yeast and humans. Notwithstanding, all centromeres function to enact spindle microtubule attachment and orchestrate precise chromosome segregation during mitosis (6,7). Neocentromeres can arise at unrelated chromosomal regions to assemble kinetochores. Thus, centromere identity is believed to be epigenetically determined (8).

The centromere-specific histone H3 variant CENP-A is accepted as the epigenetic factor that establishes the construc-

Received: May 2, 2023. **Revised:** January 24, 2024. **Editorial Decision:** January 24, 2024. **Accepted:** January 29, 2024

tion of the centromere as it is present on all functional centromeres. The central role of CENP-A is supported by an *in vitro* kinetochore assembly experiment which showed that adding reconstituted CENP-A nucleosomes to cell-free extracts was sufficient for kinetochore protein assembly, microtubule stabilization, and mitotic checkpoint protein mounting (9,10). *In vivo*, the architectural disruption of CENP-A chromatin results in compromised centromeric integrity, aneuploidy and chromosome missegregation (11,12).

The expression dosage of CENP-A appears to be important to the cell: overexpression of CENP-A is associated with its erroneous incorporation into chromosomal arm locations, which can seed kinetochore formation and result in chromosome missegregation defects, as observed in cultured cervical cancer cells and some primary colon cancer cells (13,14). Indeed, overexpression of CENP-A is associated with many cancer types and thus proposed to be a prognostic indicator of poor-survival–grade tumors and malignancy relapse (15–18).

CENP-A that has incorporated into the centromeric chromatin after DNA replication must be maintained to ensure proper construction of the kinetochore for chromosome segregation. The cell hosts numerous chaperone factors to maintain CENP-A localization at different periods within the cell cycle. Newly synthesized CENP-A first complexes with histone H4 and Scm3 in fission yeast (HJURP in mammals) via a CENP-A targeting domain (CATD) motif nested in its histone fold (19–22). In fission yeast, CENP-A associates with the NASP-like Sim3 via the N-terminal domain for handing over to Scm3/HJURP (23,24), and is then directed to centromeric chromatin via association with the Mis16-Mis18 complex in collaboration with Mis6-Mis15-Mis17-Sim4 complex (19,20,25,26). Any disruption to these loading factor complexes can deplete CENP-A at the centromere (19,20,23,24,27). Mammalian counterparts of many of these factors constitute a constitutive centromere-associated network that link the centromeric DNA to the outer kinetochore adaptor interface (28).

The centromere also hosts several factors to ensure CENP-A localization, among which is the GATA-type transcription factor Ams2 in fission yeast. This factor loads CENP-A during S-phase and in late G2 phase (29–31). Transcription-related machineries are increasingly implicated in CENP-A incorporation; albeit the mechanism is still unclarified. Treatment with transcription inhibitors can destabilize CENP-A incorporation in metazoans (32,33), and CENP-A has been reported to bind some centromere-derived transcripts, implicating transcription of underlying sequences to CENP-A centromere incorporation (32). Transcription-related processes and factors, for example, stalling of elongating RNA polymerase II (RNAPII) on centromeric locus, can encourage chromatin remodeling in favor of CENP-A incorporation in fission yeast (34), whereas RNAPII-associating Spt6 can bind to and facilitate new CENP-A incorporation at centromeres in fly (35). RNAPII-dependent transcription of centromeric sequences is associated with the removal of 'placeholder' histone H3 nucleosomes after DNA replication, which are then replaced by CENP-A at the centromere (36,37). Some studies suggest that centromeric DNA transcription is related to the initial establishment of CENP-A chromatin rather than its maintenance (38), which may explain why transcripts from CENP-A chromatin are not detected in normal asynchronously growing wild-type cells.

The detection of transcripts arising from centromeric sequences is correlated with the disruption of centromeric chromatin (24,39–42), and is probably associated with the uninhibited access of RNAPII, which disrupts the compacted chromatin of the centromere and facilitates the delocalization of centromere-associated factors including CENP-A (41). CENP-A can be delocalized from the centromere under several scenarios that may include abnormal disruption of centromere chromatin, or overexpression of CENP-A. The fate of delocalized CENP-A is not well characterized; although, a large portion of CENP-A is subjected to proteolysis (43–46). Some reports observed delocalization of overexpressed CENP-A to chromosomal arms, and the subsequent formation of an ectopic kinetochore that correlated with aneuploidy formation (13,14,47). The stochastic incorporation of CENP-A can also occur at extra-centromeric sites to form neocentromeres, particularly at that juxtaposing heterochromatin blocks (8,48,49). These findings indicate that some delocalized CENP-A could escape proteolysis to incorporate into extra-centromeric loci.

Here, we report that ribosomal DNA (rDNA) is a site of temperature-sensitive SpCENP-A$^{cnp1\text{-}1}$ mutant delocalization in fission yeast. We show that downregulation of the H3K36 methyltransferase Set2 enables the excavation of these mislocalized CENP-A at rDNA for their retargeting to the centromere. Downregulation of the *set2* directs histone chaperone Ccp1 that physically interacts with Swc2 of the SWR1 complex, to evict CENP-A from rDNA. Our results suggest Set2 coordinates a 'back-up' pathway to relocalize misincorporated CENP-A from extra-centromeric loci.

Materials and methods

Fission yeast manipulation

Basic techniques for working with *S. pombe* cells were followed (50,51). Cells were grown in YEA media (3% glucose, 0.5% yeast extract, 75 mg/l adenine) (Sigma-Aldrich; St. Louis, MO). For strains with overexpressed plasmids, Edinburgh Minimal Media (EMM) supplemented with Complete Supplement Mixture (CSM) lacking leucine (EMM-leu) (MP Biomedicals; Santa Ana, CA, USA) was used. Strains with multiple gene mutations were generated using tetrad dissection analysis, as previously described (52). Strains, plasmids, and primers used in this study are listed in Supplementary Tables S1, S2 and S3, respectively. For experiments involving both 22°C and 33°C, such as for microscopy observation of nuclear morphology or GFP foci, ChIP, reverse-transcription PCR, and immunoblot, cells were grown at 22°C and shifted to 33°C for 4 h, unless otherwise stated in the figure legend.

Spotting analysis and growth conditions

Actively growing cells were collected, concentrated to 10^7 cells/ml, and either five- or ten-fold serially diluted then spotted onto YEA plates and incubated at 26°C, 30°C, 33°C or 36°C. Cells transformed with REP41 plasmids were precultured in EMM-leu with 100 μM thiamine, washed five times with sterile water, resuspended in fresh EMM-leu without thiamine (T) and grown for at least 24 h to induce the overexpression of the *nmt41* promoter. Cells were then spotted on EMM-leu plates and incubated at the indicated temperatures. Cell growth was documented with a scanner (Epson Perfection v800 Photo) (Epson, Tokyo, Japan).

Microscopy observation

Five percent glutaraldehyde-fixed cells were stained with 4′,6-diamidino-2-phenylindole (DAPI) for observations of nuclear morphology. To observe SpCENP-A$^{cnp1\text{-}1}$ GFP foci, cells were fixed with methanol, as previously described (39,53). Cell imaging was performed on a Nikon Eclipse Ti-E fluorescence microscope and image processing performed with Nikon NIS Element AR (v5.02) (Nikon; Tokyo, Japan).

Chromatin immunoprecipitation (ChIP)

ChIP assay was performed as previously described (39,54). Cells were fixed with 3% formaldehyde and 10 mM dimethyl adipimidate (DMA). Sheared DNA was immunoprecipitated using αHA and αGFP antibodies (refer below). Competitive end-point PCR was performed by mixing primers targeting the centromeric locus *cnt1/3,* rDNA region (*rDNA*), heterochromatic *dh* domain at centromere (*cen-dh*) and subtelomere (*subtel-dh*), or the neocentromere regions (*ssp2, tel1-R, tel2-L, mat*). Primers of internal controls *act1*, or nucleosome-free region (*NFR*) were included in the same PCR reaction. PCR products were electrophoresed on agarose gels and band intensities were quantified using ImageQuant TL software (GE Healthcare, Little Chalfont, UK).

For calculation of protein enrichment on a particular locus, the following equation was used: band intensity for [locus of interest/locus of internal control] of IP divided by band intensity for [locus of interest/locus of internal control] of WCE. Samples for each trial were normalized to the respective non-treated controls (wild type (WT), 0 h or 22°C) to get relative fold enrichment (RFE) to reduce the inter-replicate variation. For calculation of qPCR-derived ChIP result, the normalized value of target locus to the internal control locus (ΔΔCt) was first calculated = $(^{Ct}\text{WCE} - {}^{Ct}\text{IP})^{\text{Internal control}} - (^{Ct}\text{WCE} - {}^{Ct}\text{IP})^{\text{Target locus}}$. Relative fold enrichment of the target locus over the internal control locus was then calculated = $2^{-\Delta\Delta Ct}$.

Reverse transcription PCR (RT-PCR) and quantitative PCR (qPCR)

Trizol reagent (Thermo Fisher Scientific, Waltham, MA) was used for the extraction of total RNA from cells, as previously described (52). DNase-treated RNA was converted to cDNA using a One-Step RT-PCR kit (Qiagen, Venlo, Netherlands). End-point RT-PCR was done using centromere targeting primers *cnt1/3*, with *act1* internal control. For validation of the RNA-seq results and ChIP of SpCENP-A$^{cnp1\text{-}1}$, qPCR was carried out using iTaq Universal SYBR Green Supermix (Bio-Rad Laboratories, Hercules, CA, USA) and the StepOne real-time PCR system (Applied Biosystems, Foster City, CA, USA), with primers amplifying gene coding sequences, *rDNA*, *cnt1/3*, with *act1* as internal control.

RNA sequencing (RNA-seq) and data analysis

DNase-treated RNA samples from wild type (WT) and *set2* mutant (*Δset2*) cells were submitted to commercial vendor for RNA-seq (BGI Genomics, Shenzhen, China) and sequenced using the Illumina HiSeqTM 2000 platform (Illumina, San Diego, CA, USA). NovoAlign (http://www.novacraft.com) was used to map the reads to the *Schizosaccharomyces pombe* (*S. pombe*) reference genome (ASM294 v2.25) to generate SAM/BAM files. *HTseq* software (version 1.0) was used to determine the gene expression levels supplied by the BAM files (55). Expression data were normalized using total mappable counts. Normalized gene expression data with >1.5-fold change (cut-off) were categorized as differentially expressed genes (DEGs). The GEO accession code of the RNA sequencing data is GSE196504.

Immunoblotting

Asynchronous cells were collected, and total protein was extracted using 20% trichloroacetic acid (Sigma-Aldrich) (71,76). Western blotting and immunostaining were carried out according to previously published procedures (24,52). The following antibodies were employed: αHA (11583816001, Roche Diagnostics, Basel, Switzerland), αGFP (1181446001, Roche Diagnostics), αFLAG (014–22383, Wako Chemicals, Osaka, Japan), αSer5P-PolII (H14, Covance, Princeton, NJ, USA), αTAT1 (56), αH3K36me2 (MABI0332, MAB Institute Inc., Kanagawa, Japan), αH3K36me3 (ab9050, Abcam, Cambridge, UK) and αCdc2 antibodies (sc-53, Santa Cruz Biotechnology, Dallas, TX, USA). Chemiluminescence signal was imaged using an ImageQuant LAS 4000 imager, with band intensities quantified using ImageQuant TL software (GE Healthcare).

Immunoprecipitation

Asynchronous cells expressing Ccp1 tagged with GFP-HA fusion (Ccp1-HA) and Set2-FLAG were collected at OD_{600nm} <1.0. Cell extracts were prepared as described previously (57), with modifications. Briefly, cells were lysed with Breaking buffer [50 mM Tris–HCl (pH 8.0), 300 mM NaCl, 1 mM MgOAc, 0.1% NP40, 0.5 mM EDTA, 10% glycerol, 2 mM PMSF, supplemented with cOmplete protease inhibitor combination (Roche Diagnostics)] and then homogenized with FastPrep-24 (MP Biomedicals, Santa Ana, CA, USA). Immunoprecipitation was performed at 4°C for 2 h with rotation using 2.4 μg of αFLAG and αHA antibodies prebound for 1 h with a 20-μl mixture of Protein A and Protein G agarose beads (Roche Diagnostics). Samples were washed 5 times with lysis buffer and the bound proteins were eluted by boiling in 2× sample buffer (0.125 M Tris, 4% SDS, 20% glycerol, 10% 2-mercaptoethanol) before immunoblotting. For co-immunoprecipitation (CoIP) between Swc2 and Ccp1, Swc2 was tagged with 3× HA (Swc2-HA) and Ccp1 was tagged with GFP (Ccp1-GFP) in the background of *Δset2cnp1-1* cells.

Phloxine B cell viability assay

Cells grew at 22°C in YEA media were shifted to 33°C for 48 h. Phloxine B (Nacalai Tesque Inc., Kyoto, Japan) was added to a final concentration of 5 μg/ml and continue incubation for an hour. Cells were then washed twice with 1× PBS and observed under fluorescence microscope. Cells that were stained red was considered as non-viable cells. Percentage (%) viability was calculated = [number of non-red stained cells/total cell counted] × 100%.

Proteasome inhibition assay

Actively growing cells with Flag-tagged Set2 were incubated with 100 μM bortezomib (LC Laboratories, Woburn, MA, USA). Control samples were treated with DMSO solvent. Cells were harvested for immunoblotting or ChIP following aforementioned procedures.

Statistical analysis

Technical triplicates of each experiment were performed, and data were analyzed using Student's *t*-test. *P* value <0.05, <0.01 and <0.005 were considered statistically significant and are represented by *, ** and ***, respectively. All statistical analyses were performed using Microsoft Excel.

Results

Deletion of *set2* restores centromeric localization of SpCENP-A$^{cnp1\text{-}1}$ to prevent chromosome missegregation

Transcription elongating machinery is implicated in regulating the centromeric incorporation of CENP-A (34,58). To study the relationship between the H3K36 methyltransferase Set2, which interacts with elongating RNAPII (59), we evaluated whether *set2* absence would aggravate the temperature-sensitive growth defects of *S. pombe* cells bearing a CENP-A (SpCENP-A) mutation, *cnp1-1*. This mutant hosts an L87Q mutation in the histone fold domain that confers temperature-sensitive centromere binding to the mutant SpCENP-A protein (12,29). We deleted *set2* (*Δset2*) in *cnp1-1* cells and studied the growth phenotypes. Instead of enhancing the *cnp1-1* growth defect, the absence of *set2* unexpectedly led to a >100-fold suppression in *cnp1-1* cell death at the restrictive temperature of 30–33°C (Figure 1A). This growth enhancement effect was accompanied by a 50.7% reduction in unequal chromosome segregation frequency in *Δset2cnp1-1* cells relative to *cnp1-1* cells (Figure 1B).

CENP-A-containing centromeric chromatin is transcriptionally silenced but becomes derepressed when *cnp1-1* is exposed to restrictive temperatures, at which SpCENP-A$^{cnp1\text{-}1}$ delocalization is correlated with unrestricted RNAPII accessibility, leading to upregulated transcription of the centromere DNA (39,40) (Figure 1C). Consistent with the suppression of chromosome missegregation, *Δset2* cells demonstrated a 3.2-fold reduction in the proportion of transcripts arising from centromeric core sequences; this pointed to restoration of centromere chromatin integrity in *cnp1-1* mutants due to the loss of *set2* (Figure 1C). This notion was further supported by a 43% restoration of centromeric spot localization patterning (Figure 1D) and a 1.8-fold increase in SpCENP-A$^{cnp1\text{-}1}$centromeric binding in *Δset2* cells (Figure 1E, *Δset2*). Finally, we showed that total protein levels of SpCENP-A$^{cnp1\text{-}1}$ were similar between WT cells and cells hosting the loss of *set2*, indicating that the restoration of SpCENP-A$^{cnp1\text{-}1}$ localization was not merely a consequence of altered protein expression (Figure 1F).

We noted that shifting to 33°C resulted in a reduction in SpCENP-A$^{cnp1\text{-}1}$ protein levels to a similar extent in both WT and *Δset2* (Figure 1F). To ensure that the decrease centromeric binding of SpCENP-A$^{cnp1\text{-}1}$ was not impacted by such reduction, we increased the protein level of SpCENP-A$^{cnp1\text{-}1}$ via overexpressing from an inducible *nmt41* promoter (41,60). Under this condition, we still observed delocalization of overexpressed SpCENP-A$^{cnp1\text{-}1}$ from the centromere upon shifting the cells to the restrictive temperature (Supplementary Figure S1A and B). Meanwhile, we also showed that overexpressed SpCENP-A$^{cnp1\text{-}1}$ did not suppress *cnp1-1* strain, but in contrast enhanced the suppression effect of *Δset2* on *cnp1-1*, linking the complementation of *cnp1-1* defect by *Δset2* to the enhanced centromeric localization of SpCENP-A$^{cnp1\text{-}1}$ (Supplementary Figure S1B and C).

H3K36 dependency in the rescue of SpCENP-A$^{cnp1\text{-}1}$ growth defects and centromeric mislocalization

H3K36 is a major downstream target of Set2-dependent methylation and, thus, we sought to investigate whether the loss of H3K36 methylation could also suppress *cnp1-1*. We created a strain that expressed histone H3 with non-methylatable K36 via incorporating a *K36R* (R:arginine) missense point mutation into all three histone H3 genes (*hht1*$^+$, *hht2*$^+$ and *hht3*$^+$) (52) in the *cnp1-1* background. Resembling *Δset2cnp1-1*, *H3K36Rcnp1-1* mutant grew better than *cnp1-1* at 30–33°C. This observation indicates that the suppression of *cnp1-1* temperature sensitive growth defect is dependent on H3K36 (Supplementary Figure S2A). The rescue of growth defect of *cnp1-1* by H3K36R was associated with the suppression of chromosome segregation defect (Supplementary Figure S2B).

Next we investigated the effect of H3K36R on centromeric localization of SpCENP-A$^{cnp1\text{-}1}$GFP, relative to *Δset2* and WT as positive and negative controls respectively. In the WT background in which *set2* and *H3K36* were not mutated, cells showing SpCENP-A$^{cnp1\text{-}1}$GFP centromeric dot decreased from 83.6% at 22°C (0 h), to 12.6% after 2 h at 33°C (Figure 2B, black bars, '+ *set2*'), whereas the strain hosting deletion of *set2* showed 99.3% and 58.1% cells with SpCENP-A$^{cnp1\text{-}1}$GFP centromeric spots at 0 and 2 h respectively (Figure 2B, grey bars, 'Δ *set2*'). Unexpectedly, H3K36R showed only about two folds more (25%) SpCENP-A$^{cnp1\text{-}1}$GFP centromeric spots at 33°C for 2 h, which was significantly lower than that in *Δset2* (Figure 2B, white bars, '*H3K36R*'). Similar trend was observed upon longer (4 h) incubation at 33°C. ChIP, however showed *H3K36R* was unable to rescue the loss of binding of SpCENP-A$^{cnp1\text{-}1}$ to *cnt1/3* centromeric DNA at 33°C, unlike *Δset2* but similar to WT background (Figure 2C). Total SpCENP-A$^{cnp1\text{-}1}$GFP protein levels were similar among the three strains, suggesting that the change in localization patterns was not a result of altered protein levels (Figure 2D).

To further ascertain that the dependency of suppression of SpCENP-A$^{cnp1\text{-}1}$GFP centromeric mislocalization on H3K36 methylation, we constructed a catalytically dead SET domain mutant of *set2*—*set2-D295AY296A*—by mutating Asp-295 and Tyr-296 to alanine. Immunoblots revealed that the incorporated mutation did not destabilize Set2 protein (Figure 2E), but compromised di- and trimethylation on H3K36 (Figure 2F). Similar to *Δset2* and *H3K36R*, *set2-D295AY296A* also suppressed *cnp1-1* temperature sensitive growth defect at 33°C (Supplementary Figure S2C), and was able to restore centromere binding defect of SpCENP-A$^{cnp1\text{-}1}$ at 33°C, like *Δset2*, but unlike *H3K36R* (Figure 2C, G). These observations taken together suggest that while the suppression of growth defect of *cnp1-1* is H3K36-dependent, the restoration of centromeric DNA binding of SpCENP-A$^{cnp1\text{-}1}$ is Set2- and SET domain-dependent but H3K36-independent.

Set2 transcriptionally represses expression of genes encoding several chromatin regulators in fission yeast

A loss-of-function of *set2* may affect global transcription. We thus performed whole-genome expression analyses to assess this possibility. We identified 15.87% of total genome to be differentially affected by *Δset2* relative to WT (Figure 3A and B). Among the 11.65% genes upregulated in *Δset2*, we noticed

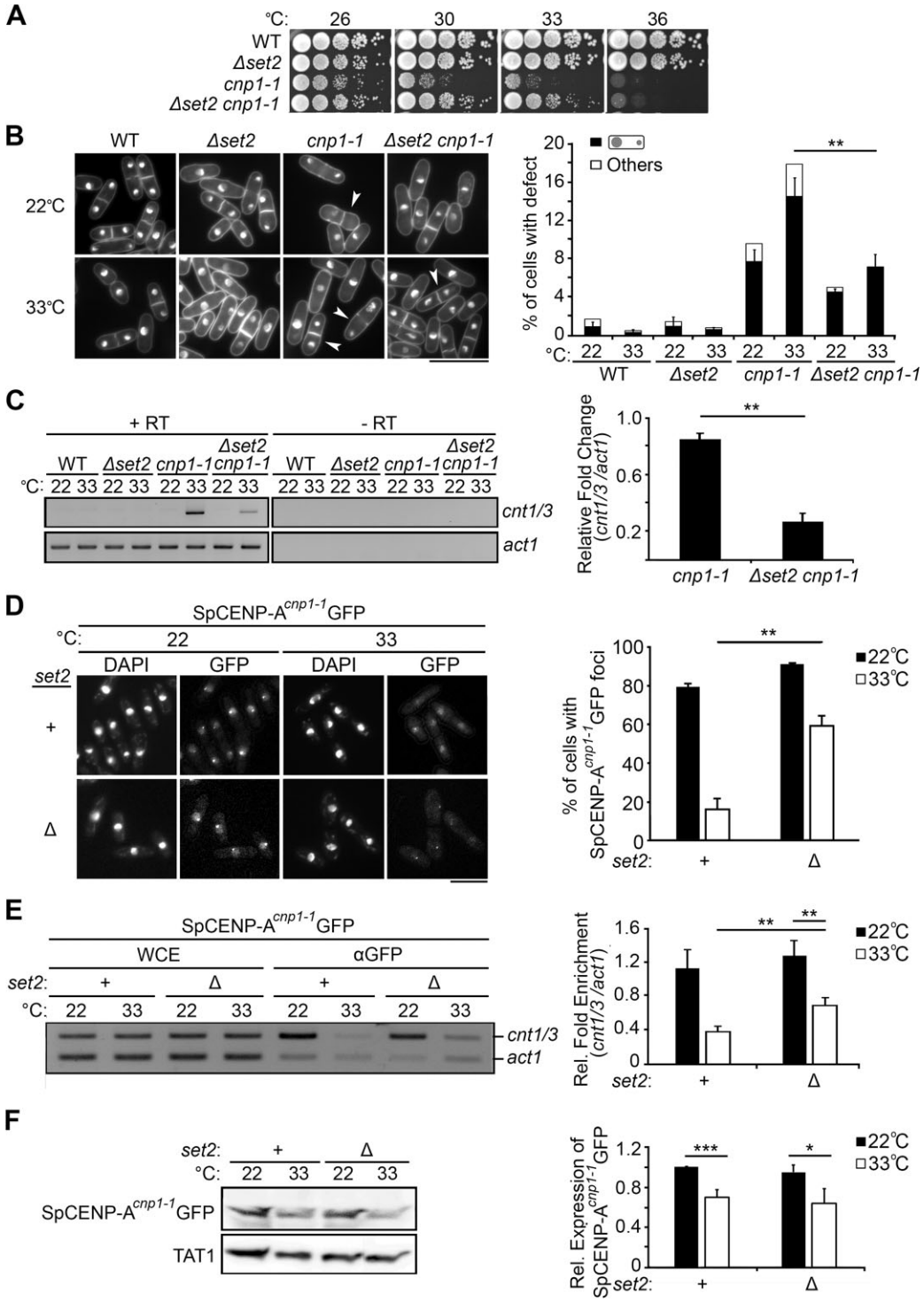

Figure 1. Downregulation of Set2 retargets delocalized CENP-A to the centromere. (**A**) The growth of wild type (WT), *set2* mutant (*Δset2*), SpCENP-A mutant (*cnp1-1*), and double mutant (*Δset2cnp1-1*) cells was ten-fold serially diluted and tested at different temperatures. (**B**) Nuclear morphology of DAPI-staining in strains grown at 22°C and 33°C. Arrowhead depicts cells with unequal chromosome segregation. Scale bar: 10 μm. Graph shows the frequency of cells with unequally segregated chromosomes (black bar) or with other aberrant nuclear morphologies (white bar). $N = 200$. Results are the mean ± S.D. of three experiments. $^{**}P < 0.01$. (**C**) RT-PCR targeted on centromeric core sequences (*cnt1/3*) for strains incubated at 22°C and 33°C, with *act1* used as the loading control. Results are representative of three experiments. –RT: no reverse transcription control. Graph shows relative fold change quantification of band intensities of *cnt1/3* transcript over *act1* from three experiments. Data represents the mean ± S.D. $^{**}P < 0.01$. (**D**) Microscopy observation of GFP-tagged SpCENP-A^{cnp1-1} and nuclear staining (DAPI) of cells in the presence (+) or absence (Δ) of *set2* at 22°C and 33°C. Scale bar: 10 μm. Graph showing quantification of SpCENP-A^{cnp1-1}GFP foci. Black bar: 22°C. White bar: 33°C. $N = 200$. Data represents the mean ± S.D. $^{**}P < 0.01$. (**E**) Competitive PCR for ChIP assay to determine the localization of SpCENP-A^{cnp1-1}GFP on the centromere core (*cnt1/3*), with *act1* as the internal control locus. WCE: whole cell extract. Graph of relative fold enrichment compares the *cnt1/3:act1* ratio for cells in the presence (+) or absence (Δ) of *set2* at 22°C and 33°C. Data represents the mean ± S.D. of three replicates. $^{**}P < 0.01$. (**F**) Expression of SpCENP-A^{cnp1-1}GFP protein in strains with (+) or without (Δ) *set2* at 22°C and 33°C, with TAT1 as the loading control. Results are representative of three experiments. Graph shows the relative expression of SpCENP-A^{cnp1-1}GFP over TAT1. Data represents the mean ± S.D. $^{*}P < 0.05$. $^{***}P < 0.005$.

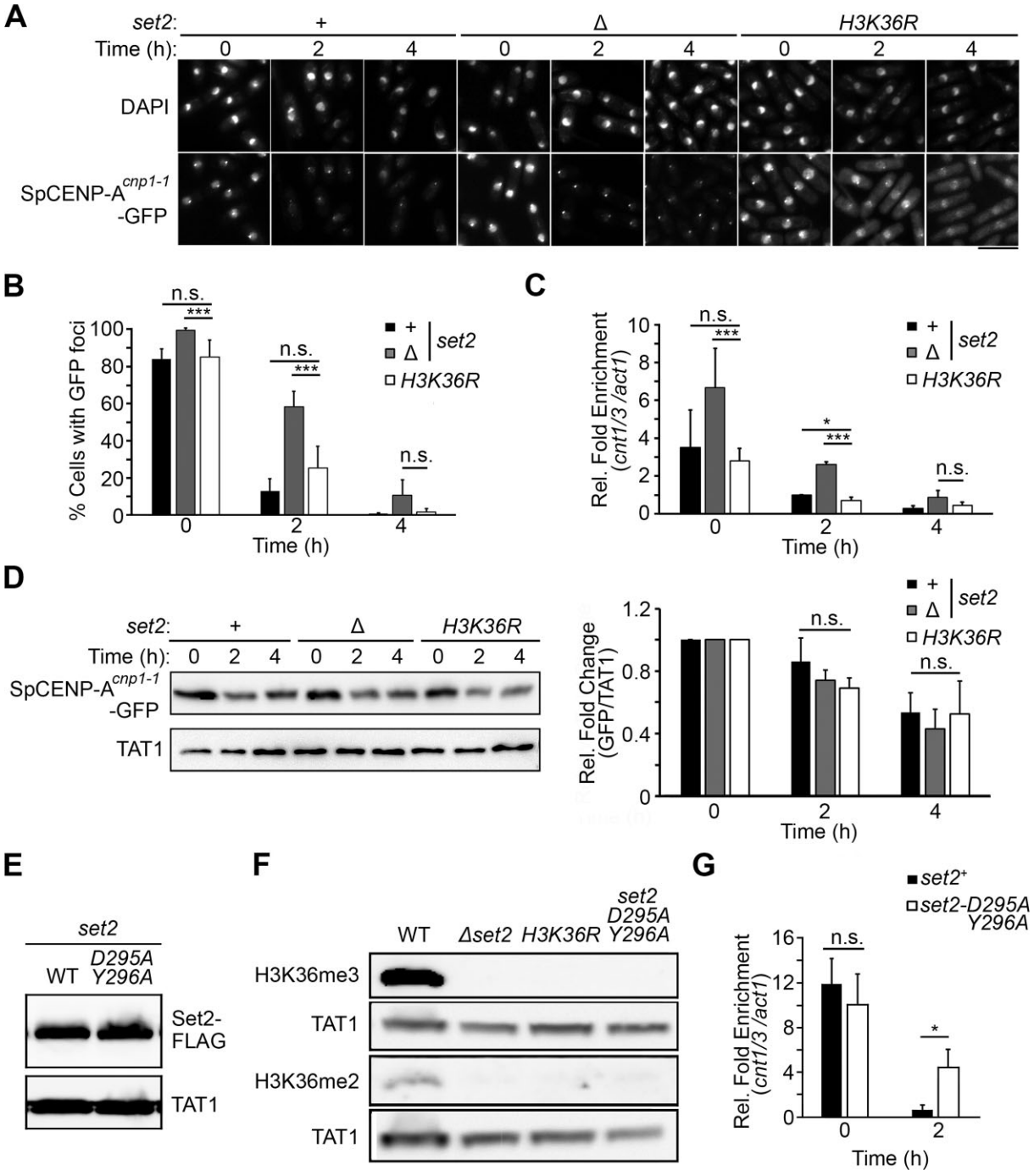

Figure 2. Effect of H3K36 and catalytic activity of Set2 SET domain on *cnp1-1* suppression. (**A**) Microscopy observation of GFP-tagged SpCENP-A^{cnp1-1} and nuclear staining (DAPI) of cells in the presence (+) or absence (Δ) of *set2* and the H3K36R mutant incubated at 22°C (0 h) and 33°C for 2 and 4 h. Scale bar: 10 μm. (**B**) Graph shows the quantification of cells with SpCENP-A^{cnp1-1}GFP foci. $N = 200$. Error bars represent the mean ± S.D. of three replicates. $***P < 0.005$. n.s., not significant. (**C**) qPCR for ChIP of SpCENP-A^{cnp1-1}GFP at the centromere region (*cnt1/3*) with *act1* as the internal control locus for strains incubated at 33°C for the indicated timeframes. $*P < 0.05$. $***P < 0.005$. n.s., not significant. (**D**) Protein expression of SpCENP-A^{cnp1-1}GFP in the presence (+) or absence (Δ) of *set2*, and H3K36R cells incubated for different durations (h) at 33°C. TAT1 was used as the loading control. Results are representative of three experiments. Graph shown is the mean ± S.D. $N = 3$. n.s., not significant. (**E**) Protein expression of FLAG-tagged wild type Set2 and catalytic-dead mutant (*set2-D295AY296A*) with TAT1 as loading control. (**F**) Levels of H3K36 di- (me2) and tri- (me3) methylation was tested by immunoblotting in WT, *Δset2*, H3K36R and catalytic-dead mutant of Set2 (*set2-D295AY296A*) with TAT1 as the loading control. (**G**) qPCR for ChIP of SpCENP-A^{cnp1-1}GFP at the centromere region (*cnt1/3*) with *act1* as the internal control locus for strains incubated at 22°C (0 h) and 33°C for 2 h. $*P < 0.05$. n.s., not significant.

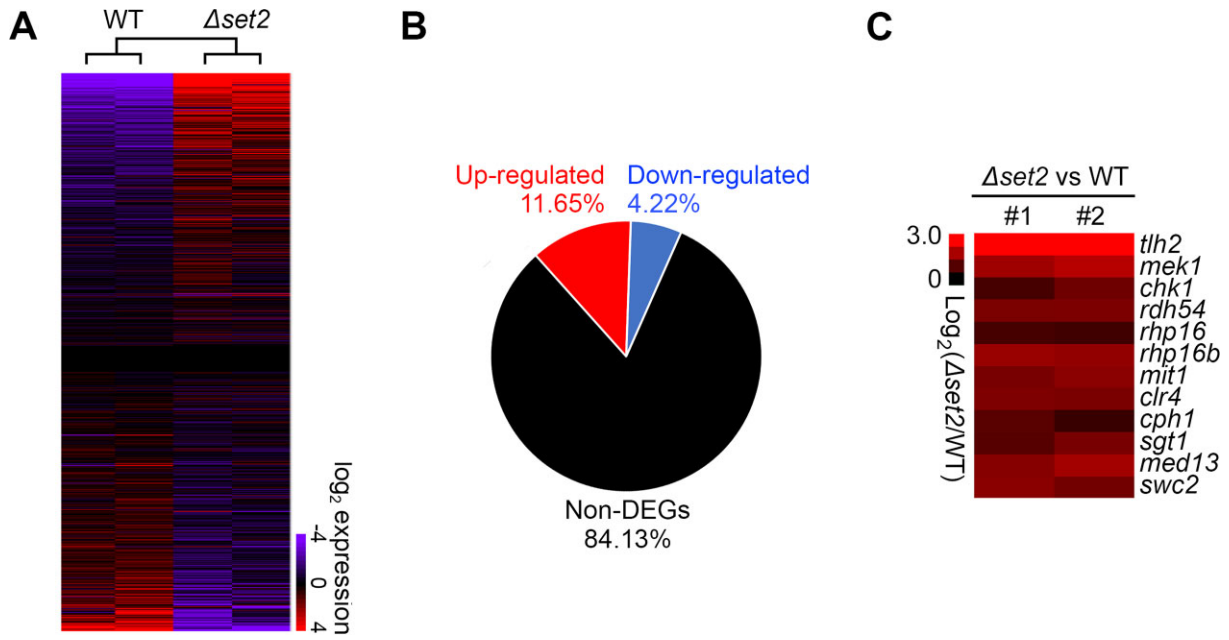

Figure 3. Set2 transcriptionally represses the expression of several chromatin regulators. (**A**) Hierarchical clustering of genes from the genome-wide gene expression profiles of WT and *Δset2* in duplicates. The heatmap is generated based on log_2-normalized values subtracted from the means of WT and *Δset2* replicates. Red and blue colors indicate upregulation and downregulation of expression respectively, whereas black indicates unchanged expression. (**B**) Pie-chart demonstrating the percentage of non-differentially expressed genes (non-DEG) as well as up- and down-regulated genes in *Δset2* versus WT cells. Genes with reproducible change in the same direction in both replicates are considered as differentially expressed genes (DEG). (**C**) Heatmap of a few representative DEGs upregulated in *Δset2* versus WT upon the deletion of *set2*.

that many of the genes encoded for chromatin factors that function in DNA damage response, heterochromatin regulation, and chromatin remodeling (Figure 3C). qRT-PCR confirmed at least a 1.5-fold upregulation in expression when *set2* was deleted (Supplementary Figure S3), suggesting that Set2 represses the transcription of these genes.

Swc2 serves as a downstream effector of *Δset2* in *cnp1-1* suppression

We considered the possibility that one or more of these Set2-repressed genes may be involved in the suppression of *cnp1-1* cell death in *Δset2*. We surmised that such a factor would need to fulfill two criteria: (i) its overexpression would suppress *cnp1-1* in a manner reminiscent of *Δset2* and (ii) its deletion would counteract the ability of *Δset2* to suppress *cnp1-1*. Among the genes tested (*rdh54, chk1, tlh2, mit1, clr4, rhp16b* and *swc2*), we noticed that overexpression of *swc2*$^+$, *clr4*$^+$ and *rhp16b*$^+$ could suppress *cnp1-1* (Figure 4A, Supplementary Figure S4). However, when these genes were deleted in *Δset2cnp1-1* background, only *Δswc2* could counteract the suppression of *cnp1-1* by *Δset2* (Figure 4C, Supplementary Figure S5). Thus, only *swc2*$^+$ fulfilled both criteria of being the downstream effector mediating suppression of *cnp1-1* by *Δset2*.

The *swc2*$^+$ gene encodes a subunit of the SWI2/SNF2-related 1 chromatin remodeling complex (SWR1-C), which catalyzes the chromatin incorporation of the histone H2A.Z variant. Swc2 is the DNA-contacting sub-unit that positions SWR1-C onto chromatin localities (61). Besides *swc2*$^+$, we confirmed that the expression of genes encoding for other subunits of SWR1-C were not upregulated in *Δset2*, including the catalytic subunit *swr1*$^+$ (Supplementary Figure S6A). Transcriptional upregulation of *swc2*$^+$ was also accompanied by an increase in Swc2 protein expression (Supplementary Figure S6B and C).

To test whether *swc2*$^+$ expression was H3K36 methylation-dependent, transcription levels of *swc2*$^+$ were assessed in *Set2-D295AY296A* and H3K36R. The *set2-D295AY296A* strain exhibited increased *swc2*$^+$ level as in *Δset2*, whereas *swc2*$^+$ level remained unelevated in the H3K36R strain, similar to the WT condition (Supplementary Figure S7A). The *swr1*$^+$ gene expression was employed as a control, which remained unchanged in *Δset2* as well as *Set2-D295AY296A* and H3K36R cells (Supplementary Figure S7B). This observation suggests that transcriptional upregulation of *swc2*$^+$ is dependent on Set2 and its catalytic activity, but unexpectedly independent of H3K36.

To further ascertain whether Swc2 may mediate the *cnp1-1* suppression by *Δset2*, we overexpressed *swc2*$^+$ in *cnp1-1* and *Δset2cnp1-1*, using the inducible *nmt41* promoter (41,62) (Supplementary Figure S8). Overexpression of *swc2*$^+$ resulted in approximately 25-fold suppression of *cnp1-1* at the restrictive temperature of 33°C relative to the vector control, as observed previously (Figure 4A). Consistent with Swc2 in mediating *cnp1-1* suppression by *Δset2*, *swc2*$^+$ expression in the *Δset2cnp1-1* double mutant did not further augment suppression of the growth defect of *cnp1-1* by *Δset2* (Figure 4A), nor resulted in further increase in Swc2 expression in the absence of *set2* (in *Δset2cnp1-1*) over that when Set2 is present (in *cnp1-1*) (Supplementary Figure S8). Microscopy analysis revealed that overexpression of *swc2*$^+$ also resulted in suppression of the chromosome segregation defects of *cnp1-1* by 23.13% at 33°C (Figure 4B). The reversal of *Δset2* suppression of *cnp1-1* growth defects by *swc2* deletion (approximately 25-fold, Figure 4C) appeared to be partial, suggesting involvement of other cooperating factors. Taken together, these observations point to Swc2 as a downstream effector

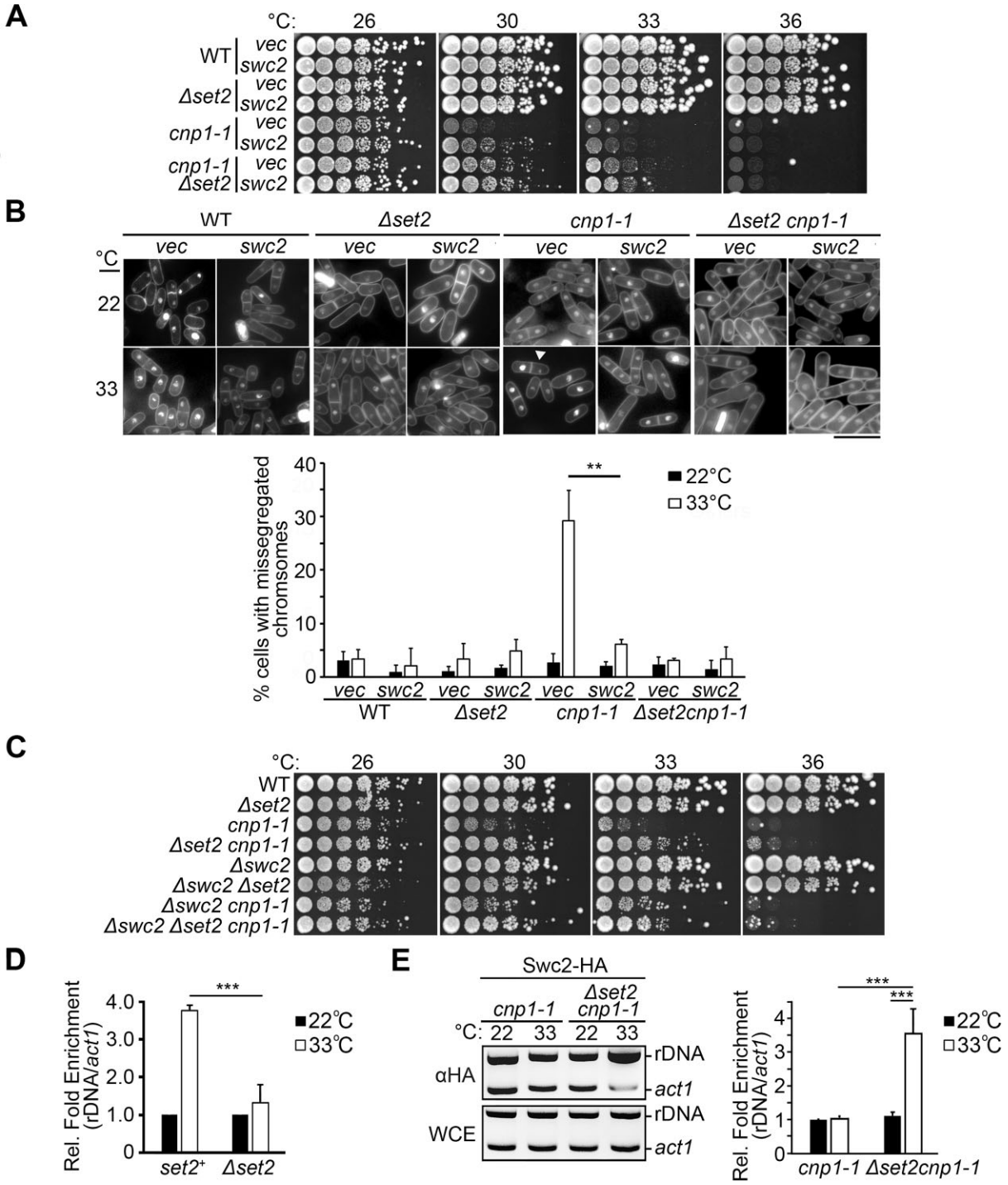

Figure 4. Swc2 suppresses chromosomal missegregation of *cnp1-1* by counteracting the mistargeting of SpCENP-A^{cnp1-1} to rDNA. (**A**) Growth of cells transformed with either vector (*vec*) or HA-tagged Swc2 plasmid and induced by the *nmt41* promoter (*swc2*). Cells were five-fold serially diluted and growth was tested at different temperatures. (**B**) Nuclear morphology of DAPI-stained strains overexpressed with vector (*vec*) or Swc2 (*swc2*) and grown at 22°C and 33°C. Arrowhead depicts cells with unequal chromosome segregation. Scale bar: 10 μm. Graph shows the frequency of cells with unequally segregated chromosomes in the indicated strains. $N = 200$. Results are the mean ± S.D. of three experiments. ** $P < 0.01$. (**C**) Growth of strains containing different combinations of *swc2*, *set2* and *cnp1-1* mutations were five-fold serially diluted and tested under different temperatures. (**D**) qPCR for ChIP of SpCENP-A^{cnp1-1}GFP at the rDNA region with *act1* as the internal control locus in cells with (+) or without (*Δ*) *set2* incubated at 22°C and 33°C. Fold enrichment is calculated relative to 22°C. $N = 3$. *** $P < 0.005$. (**E**) Competitive PCR for ChIP of 3 × HA-tagged Swc2 in *cnp1-1* and *Δset2cnp1-1* backgrounds at 22°C and 33°C. Localization of Swc2 at rDNA was tested with *act1* as an internal control locus. The figure is representative of three experiments. WCE: whole cell extract. Graph of relative fold enrichment was calculated by comparing the *rDNA*:*act1* ratio between αHA and WCE. *** $P < 0.005$.

of *Δset2* that contributes to the restoration of centromeric chromatin integrity and chromosome segregation fidelity in *cnp1-1*.

Next, we sought to explore the mechanism by which Swc2 regulates SpCENP-A centromeric localization. We considered the possibility that Swc2 may localize to centromeric loci to enhance the incorporation of SpCENP-A^{cnp1-1}. However, we were unable to reliably demonstrate direct centromere binding of Swc2 using chromatin immunoprecipitation (ChIP) after repeated efforts (Supplementary Figure S9). We then considered that Swc2 may aid in redirecting SpCENP-A^{cnp1-1} from other chromosomal loci back to the centromere in *Δset2*. Several ectopic sites are reportedly bound by SpCENP-A, including euchromatic neo-centromere formation sites that lie adjacent to constitutive heterochromatin and ribosomal DNA (rDNA) clusters (49,63). We checked the localization of SpCENP-A^{cnp1-1} using ChIP at these loci (49,63), but did not observe enrichment of SpCENP-A^{cnp1-1} using ChIP at subtelomeric regions (*tel1-R* and *tel2-L*), mating-type loci and internal regions containing the *ssp2*$^+$ gene, or at constitutive heterochromatin loci at 33°C (Supplementary Figure S10). However, we detected a 3.77-fold enrichment in SpCENP-A^{cnp1-1} on the rDNA sequence at 33°C relative to the control *act1*$^+$ site (Figure 4D, Supplementary Figure S1D). The rDNA binding of SpCENP-A^{cnp1-1} was Set2-dependent and the enrichment was compromised in *Δset2* cells (Figure 4D). Furthermore, we observed an increased occupancy of Swc2 at rDNA chromatin preferentially in the *Δset2* background (Figure 4E).

Release of centromeric Ccp1 to rDNA to destabilize mislocalized SpCENP-A^{cnp1-1}

A previous work reported that overexpressed SpCENP-A can accumulate to the rDNA region and a nucleosome assembly protein (NAP) Ccp1 is important for antagonizing such mislocalization of overexpressed SpCENP-A at rDNA (64). Ccp1, however, localizes to the centromere and it was unclarified how it regulates SpCENP-A eviction at rDNA sites (63,64). We hypothesized that Ccp1 may be targeted to rDNA in *Δset2* to excavate SpCENP-A^{cnp1-1} perhaps by collaborating with Swc2. To ascertain the relationship between Swc2, Ccp1, Set2 and SpCENP-A, we began by adopting a genetic interaction analysis using strains in which these factors were deleted singly, doubly, and triply in *cnp1-1* and assessing the effect of Swc2 and Ccp1 on the suppression of the *cnp1-1*-associated growth defect by *Δset2*. In the absence of either *ccp1* or *swc2*, we observed aggravation of the growth defect in *Δset2cnp1-1* cells. Combined deletion of both *ccp1* and *swc2* did not further compromise the ability of *Δset2* to suppress the *cnp1-1* growth defect, suggesting that Ccp1 and Swc2 function in the same epistasis group to mediate rescue of *cnp1-1* via downregulation of *set2* (Figure 5A, Supplementary Figure S11).

Genetic interaction between the factors and the effect of the mutations on the centromeric localization of SpCENP-A^{cnp1-1}GFP was supported by microscopy observations. SpCENP-A^{cnp1-1}GFP showed the characteristic centromeric spot pattern (12,29,39) in 72.4% of the cells at 22°C that was reduced to 21.5% at 33°C, and in turn restored in 65.3% of the cells after deletion of *set2*. Deletion of *swc2* or *ccp1* reduced the proportion of cells showing centromere spot localization to 48.9% and 41.9%, respectively (Figure 5B, Supplementary Figure S12). Concurrent deletion of *swc2* and *ccp1* in *Δset2* (*Δswc2Δccp1Δset2*) resulted in 31.6% centromere spot localization, which was statistically similar to *Δccp1Δset2*. Taken together, these findings indicate that Set2, Ccp1 and Swc2 function in the same epistasis group to ensure SpCENP-A centromeric localization.

We investigated whether localization of Swc2 and Ccp1 may be reciprocally affected by each other at the rDNA locus. We fused an epitope tag at the endogenous chromosomal loci of *swc2*$^+$ in *Δccp1*, and an epitope-tagged chromosomal copy of *ccp1*$^+$ gene in *Δswc2* to perform ChIP. Ccp1-GFP and Swc2-HA were targeted to rDNA at 33°C where SpCENP-A^{cnp1-1} localized (Figure 4D). However, rDNA binding of both factors was compromised in the reciprocal deletion of one or the other (Figure 5C and D). Through further immunoprecipitation experiments, we detected a physical interaction between Swc2 and Ccp1 in *Δset2* cells (Figure 5E), suggesting that Swc2 and Ccp1 were targeted to the rDNA in *Δset2* where they co-stabilized each other probably via complex formation.

We next asked whether centromere localization of Ccp1 might be affected by Set2 in *cnp1-1* in conjunction with targeting of Ccp1 to the rDNA. We therefore studied the binding of Ccp1 at rDNA and centromeric sequences in WT, *Δset2*, *cnp1-1* and *Δset2cnp1-1* cells at 33°C and at 22°C with ChIP. The levels of Ccp1 at rDNA were similar among *cnp1-1, Δset2* and WT at 33°C. However, when *set2* function was attenuated in the *cnp1-1* background, Ccp1 levels at rDNA were enriched > 2.7-fold (Figure 6A). On the other hand, Ccp1 centromere binding was abolished in *Δset2* and *Δset2cnp1-1* (0.52-fold and 0.49-fold reductions respectively) conditions (Figure 6B); albeit the protein expression of Ccp1 remained unchanged (Figure 6C).

Although the centromeric accumulation of Ccp1 was also reduced in the *Δset2* single mutant, there was no corresponding increase in Ccp1 binding at the rDNA locus; this suggested that Ccp1 can still be sequestered, and the delocalization of SpCENP-A^{cnp1-1} to rDNA could then summon Ccp1 in the absence of *set2*. From these observations, we posited that Set2 and SpCENP-A anchor Ccp1 to the centromeric reservoir. A downregulation or loss of *set2* then permits targeting of Ccp1 to rDNA. Consistent with this view, we noted the physical interaction between Set2 and Ccp1; albeit, only low amounts of Ccp1 co-immunoprecipitated with Set2, perhaps suggesting that Ccp1 only physically interacts with a small proportion of the total Set2 protein (Figure 6D).

Set2 associates with centromere core region

To prove that Set2 is indeed present at the centromere, we set out to ChIP Set2 in asynchronous cultures. However, we were unable to observe Set2 enrichment at the centromere. Budding yeast Set2 and human SETD2 proteins have elsewhere been reported to be subjected to proteasome-dependent degradative turnover (65,66), and this motivated us to consider that our inability to detect Set2 at the centromere could be attributed to its high turnover rate. Hence, we repeated the ChIP after treating cells with the proteasome inhibitor, bortezomib (67). Upon treatment with bortezomib, total Set2 level gradually increased over time (Supplementary Figure S13A). With stabilization of Set2 protein levels, we were able to detect enrichment of Set2 at the centromere locus compared to control samples treated with DMSO (Supplementary Figure S13B), thus lending support to the aforementioned anchoring role of Set2 on Ccp1 at the centromere.

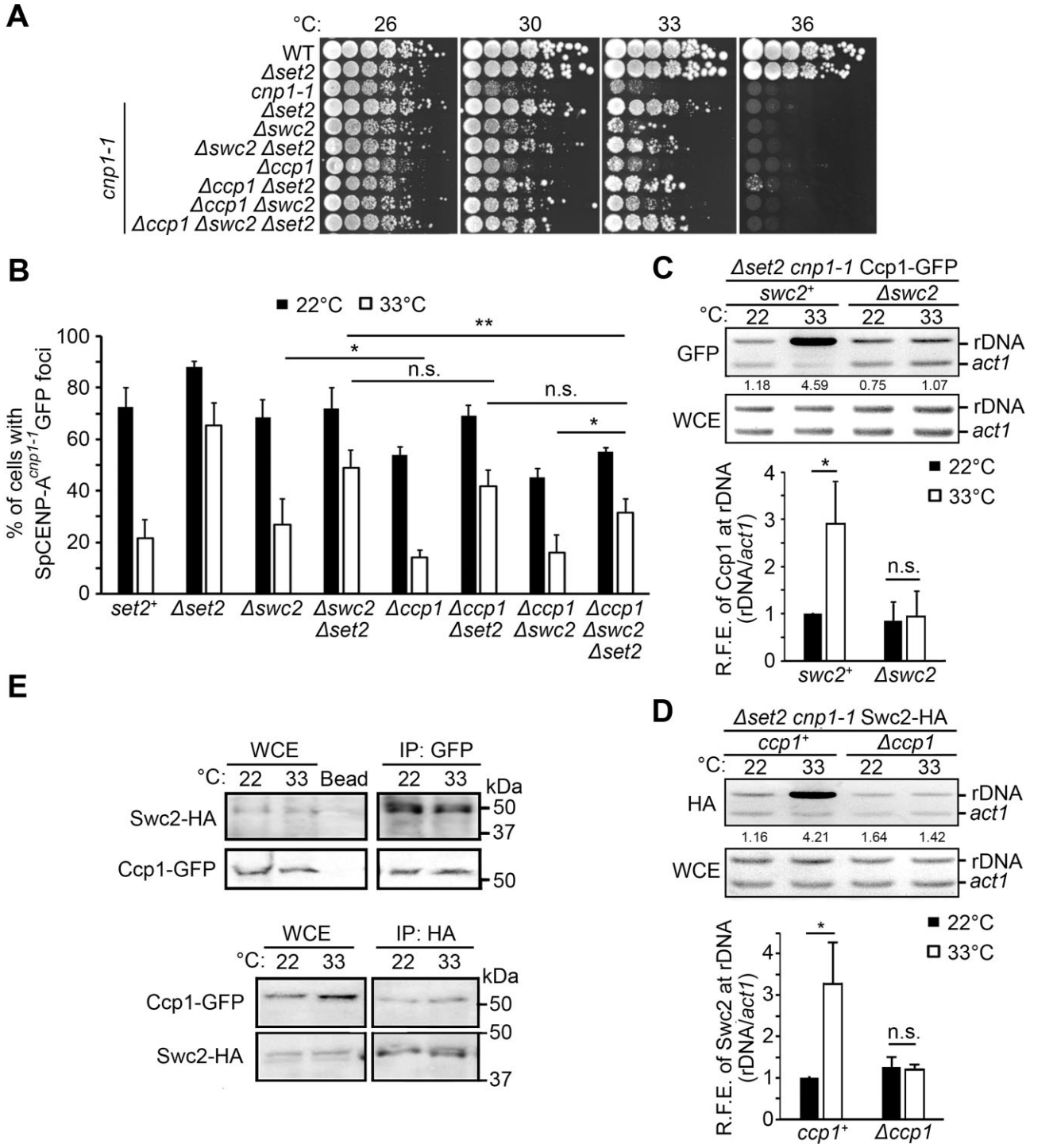

Figure 5. Swc2 interacts with Ccp1 for targeting to rDNA. (**A**) Growth of strains containing different combinations of *swc2*, *ccp1*, *set2* and *cnp1-1* mutations were five-fold serially diluted and treated under different temperatures. (**B**) Graph shows the quantification of SpCENP-A^{cnp1-1}GFP foci in different mutant cells at 22°C (black) and 33°C (white). $N = 200$. Error bars represent the mean ± S.D. of three replicates. * $P < 0.05$, ** $P < 0.01$. n.s., not significant. Competitive PCR for ChIP of (**C**) Ccp1-GFP or (**D**) Swc2-HA in the presence (+) or absence (Δ) of each other in the *Δset2cnp1-1* background at 22°C and 33°C. Localization of Ccp1 or Swc2 at rDNA was tested with *act1* as an internal control locus. The figure is representative of three experiments. WCE: whole cell extract. Graph in lower panel of (C) and (D) consolidates the respective relative fold enrichment (R.F.E.) by comparing the *rDNA*:*act1* ratio between Swc2-HA or Ccp1-GFP and WCE, in presence and absence of the reciprocal factor. *, $P < 0.05$. n.s., not significant. (**E**) Co-immunoprecipitation of Ccp1-GFP and Swc2-HA in *Δset2cnp1-1* cells treated at 22°C and 33°C. IP: immunoprecipitation. WCE: whole cell extract. Bead: beads control.

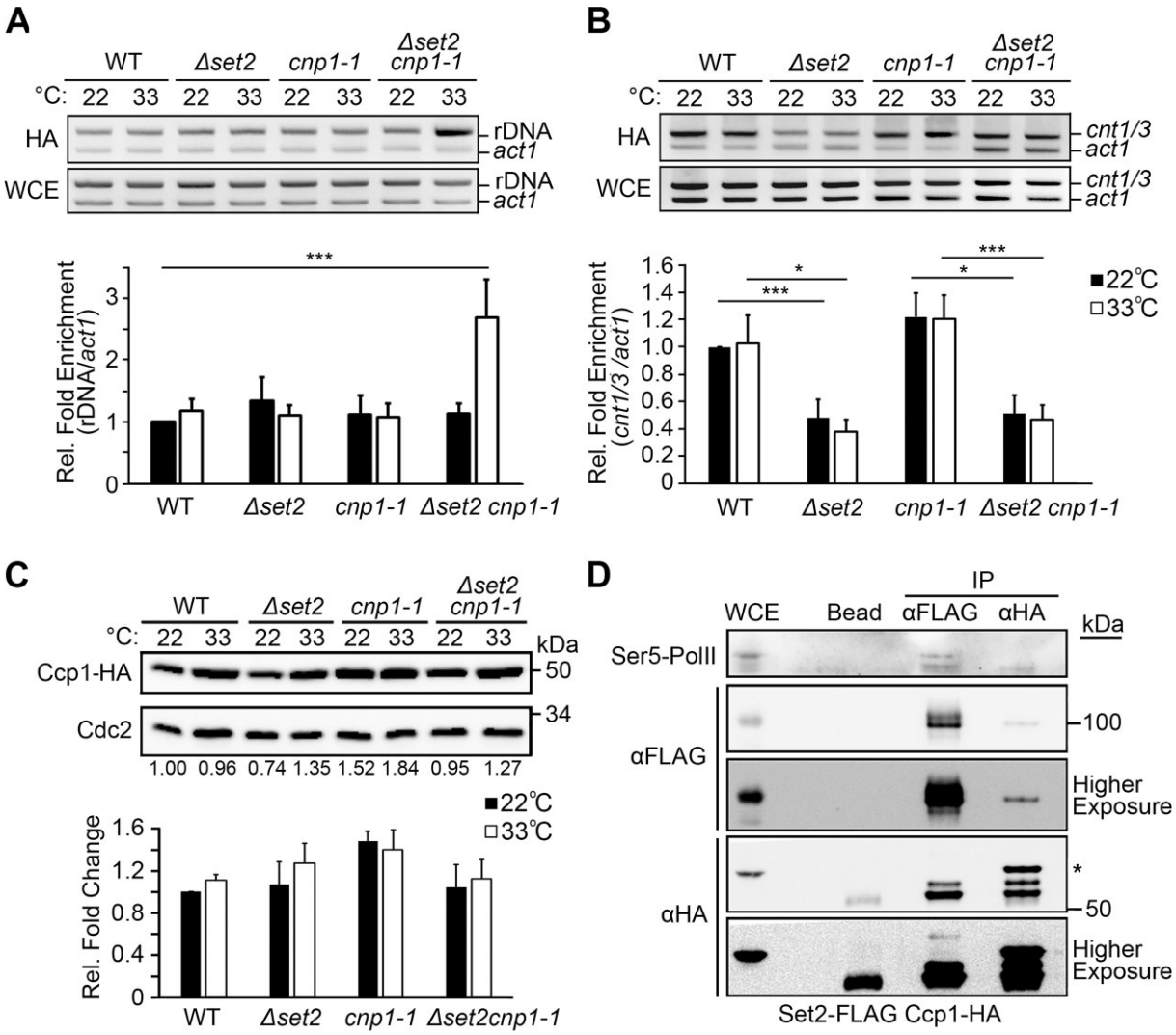

Figure 6. Set2 and SpCENP-A synergistically sequester Ccp1 at the centromere and counteract its targeting to rDNA. Competitive PCR for ChIP assay to determine the localization of 3 × HA-tagged Ccp1 (HA) in different strain background at (**A**) rDNA and (**B**) centromere core (*cnt1/3*), with *act1* as the internal control. WCE: whole cell extract. Graphs show relative fold enrichment comparing the rDNA or *cnt1/3* over *act1* ratio for cells grew at 22°C and 33°C. $N = 3$. * $P < 0.05$. *** $P < 0.005$. (**C**) Expression of Ccp1-HA protein in strains of different backgrounds incubated at 22°C and 33°C, with Cdc2 as the loading control. Results are representative of three experiments. Data represents the mean ± S.D. (**D**) Co-immunoprecipitation of Ccp1-HA and Set2-FLAG in asynchronous cultures. Phosphorylated Ser5 of RNA polymerase II (Ser5-PolII) is the positive control for Set2-FLAG IP. IP: immunoprecipitation. WCE: whole cell extract. Bead: beads control. Asterisk, Ccp1 band.

SpCENP-A loading factors reload rDNA-evicted SpCENP-A back to the centromere

A question arose as to whether the centromere relocalization of SpCENP-A$^{cnp1\text{-}1}$ in *Δset2* may also involve other SpCENP-A loading factors. We tested whether *Δset2* was able to also suppress the temperature-sensitive growth defect of mutants of centromere-binding factors that belonged to essential SpCENP-A loading complexes: *mis15-68*, *mis16-53*, *mis17-362*, *scm3-6*, *scm3-19* and *mis18-818*. Mutant of Mis14, *mis14-276*, which function independently of SpCENP-A loading pathway was used as negative control (27). The mutation of these loading factors (except *mis14-276*) disrupts centromere binding of SpCENP-A (19,20,27). *Δset2* showed prominent suppression of the growth defects of *mis16*, *mis17* and *mis18* mutants at restrictive temperatures, but at best only marginally complemented *scm3-6* and *scm3-19*. Among these, *mis17-362* appeared to be the strongest with >1000 fold suppression (Figure 7A, Supplementary Figure S14). *Δset2* was however unable to complement the temperature-dependent growth defect of *mis14-276* and *mis15-68* (Supplementary Figure S15).

Finally, to construct an alternative system besides using *cnp1-1* to show the rescue of SpCENP-A delocalization by *Δset2*, we fused a GFP tag to WT SpCENP-A in the *mis17-362* mutant. Shifting the mutant to the restrictive temperature of 33°C led to SpCENP-A mislocalization, with an increase in the number of cells exhibiting two or more SpCENP-A-GFP foci (18.2% and 3.8% at 33°C and 22°C, respectively) and a reduction in the proportion of cells with one SpCENP-A-GFP spot (69.1% and 85.0% at 33°C and 22°C respectively) (Figure 7B). Deletion of *set2* reduced cells with multiple foci and restored cells with single foci at 33°C. We also performed ChIP to assess the localization of SpCENP-A-GFP at centromere and rDNA sequences, and observed a 0.46-fold reduction in SpCENP-A-GFP centromeric localization accompanied by a

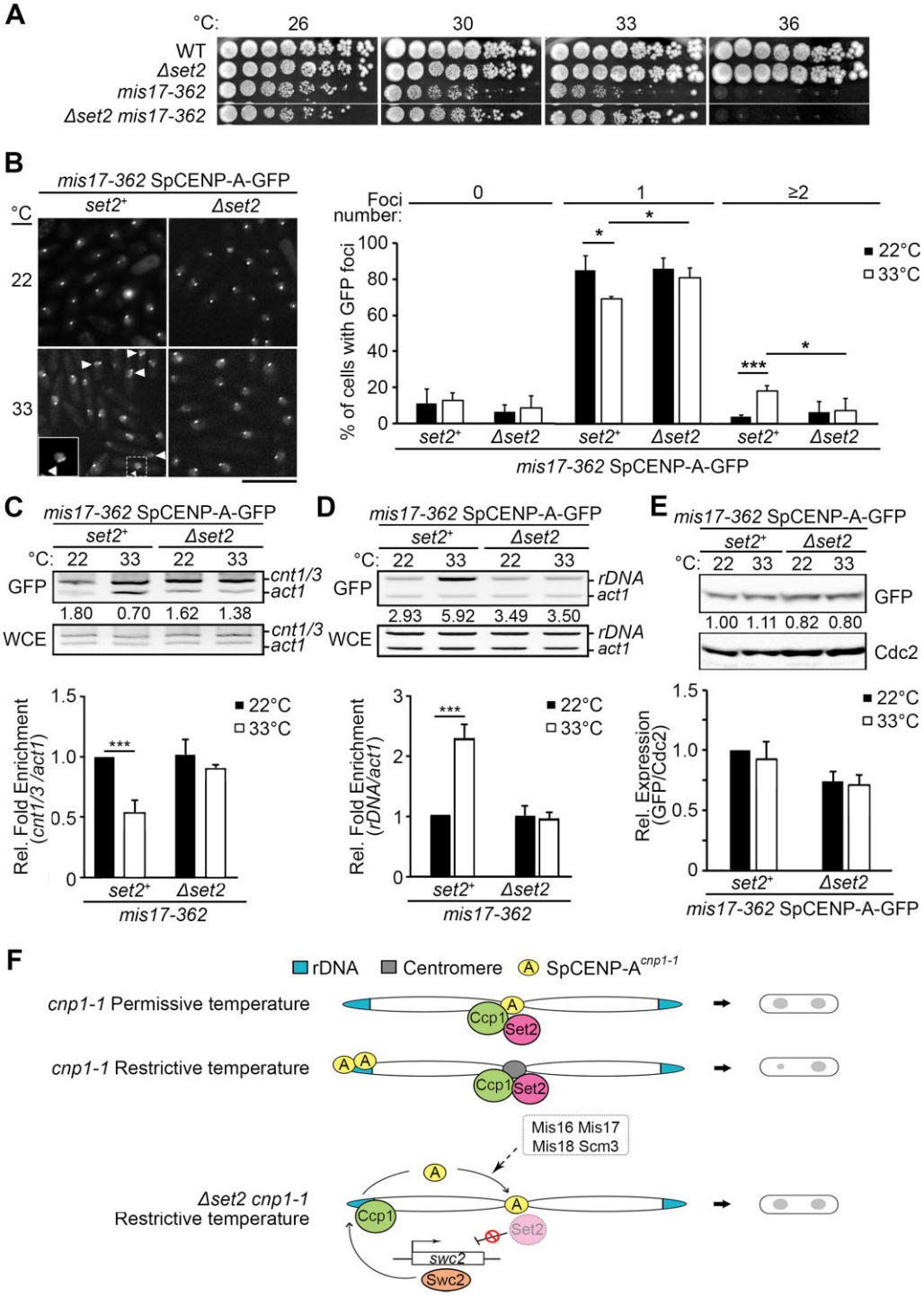

Figure 7. Mis17 cooperates with Set2 to rescue centromeric localization of mislocalized SpCENP-A. (**A**) The growth of WT, single *set2* null (*Δset2*), and *mis17-362*, and double (*Δset2mis17-362*) mutant cells were five-fold serially diluted and tested at different temperatures. (**B**) Microscopy observation of *mis17-362* cells bearing GFP-tagged SpCENP-A in the presence (*set2*$^{+}$) or absence of *set2* (*Δset2*) at 22°C and 33°C. Arrowheads, nuclei with multiple SpCENP-A-GFP dots. One such nucleus (dotted line box) was enlarged to show in the insert at the corner. Scale bar: 10 μm. Graph showing quantification of SpCENP-A-GFP foci. Black bar: 22°C. White bar: 33°C. $N = 200$. Data represents the mean ± S.D. * $P < 0.05$. *** $P < 0.005$. ChIP assay followed by competitive PCR quantification of SpCENP-A-GFP enrichment at (**C**) centromere (*cnt1*/3) and (**D**) rDNA of strains with different backgrounds incubated at 22°C and 33°C, with *act1* as an internal control locus. *** $P < 0.005$. (**E**) Protein expression level of SpCENP-A-GFP in *mis17-362* cells in the presence (+) or absence (Δ) of *set2* at 22°C and 33°C, with Cdc2 as the loading control. $N = 3$. (**F**) Model of Set2 regulation of the feedback pathway to ensure centromeric retargeting of mislocalized CENP-A in fission yeast. Under the permissive temperature, Ccp1 is sequestered to the centromere by interacting with SpCENP-A$^{cnp1\text{-}1}$ and Set2, leading to equal segregation of the chromosomes during mitosis. However, at restrictive temperatures, SpCENP-A$^{cnp1\text{-}1}$ is mislocalized from the centromere to rDNA regions while Ccp1 remains bound to the centromere by Set2. The loss of SpCENP-A$^{cnp1\text{-}1}$ destabilizes the centromere and leads to a chromosome missegregation defect. Downregulation of Set2 rescues the chromosome missegregation defect by releasing Ccp1 to the rDNA region while simultaneously derepressing *swc2* transcription. Overexpressed Swc2 is enriched at the rDNA region and cooperates with Ccp1 in promoting the centromere relocalization of SpCENP-A$^{cnp1\text{-}1}$. rDNA-evicted SpCENP-A$^{cnp1\text{-}1}$ relocalizes to the centromere with the help of SpCENP-A loading factors such as Mis16, Mis17, Mis18 and Scm3.

2.3-fold increase in SpCENP-A-GFP at rDNA (Figure 7C and D, *set2*$^{+}$). Interestingly, the level of SpCENP-A-GFP at the centromere was restored and that at rDNA reversed to the same level as that observed in permissive conditions at 33°C when *set2* is deleted in *mis17-362* cells. These observations are consistent with the restoration of SpCENP-A-GFP centromeric localization by *Δset2* in the *mis17-362* mutant, via centromeric retargeting of the SpCENP-A-GFP that was mislocalized to rDNA locus (Figure 7C and D). The observed localization change is independent of the changes in SpCENP-A protein level (Figure 7E). These results thus confirm the role of *set2* downregulation in maintaining SpCENP-A centromeric localization through reversal of the SpCENP-A misincorporation at the rDNA region.

Discussion

The incorporation of CENP-A triggers the assembly of specialized chromatin essential for kinetochore assembly and the orchestration of chromosome segregation (9,12). The mislocalization of CENP-A into non-centromeric loci, which has been observed during CENP-A overexpression and carcinogenesis, is associated with defective kinetochore microtubule attachment and aneuploidy (13,47). Hence proper targeting of CENP-A specifically to the centromere and reversal of misincorporation at non-centromeric loci are essential for the survival of the cell. Here, we identified a CENP-A-relocalizing mechanism that can reverse the mislocalization of SpCENP-A to rDNA locus. This mechanism centers on the methyltransferase Set2, which confers a two-prong pathway involving release of the Ccp1 NAP from the centromere and overexpression of SWR1 complex factor Swc2. Via complex formation, Ccp1 and Swc2 are co-targeted to the rDNA to displace the mislocalized SpCENP-A, which is then relocalized to the centromere via SpCENP-A-loading proteins including Mis17, and Mis16–Mis18 (Figure 7F).

The mis-incorporation of CENP-A to non-centromeric loci is largely prevented by proteolysis of mislocalized CENP-A, as reported in budding yeast but also in fly and human cells (45,46,68,69). We also showed that mislocalized SpCENP-A$^{cnp1\text{-}1}$ was liable to proteolysis, which contributed to the removal of the large proportion of delocalized SpCENP-A, probably to prevent mistargeting to the arm regions. The mechanism regulated by Set2, Ccp1 and Swc2 described herein can serves as a 'back-up' homeostatic response to the remaining mislocalized SpCENP-A not degraded by the proteasome.

The incomplete reversion of *Δset2* suppression of *cnp1-1* upon *swc2* and *ccp1* disruption points to the presence of addition factors that synergize with Swc2 and Ccp1 to relocalize SpCENP-A$^{cnp1\text{-}1}$. Recent research revealed that SpCENP-A loading is a multistep process that involves not only the actual packaging of the histone variant-containing nucleosome into the centromeric DNA, but also entails ushering of the SpCENP-A into the centromeric vicinity apparently constituting a cloud of concentrated SpCENP-A and associated histone chaperones (24). One such location is shown to juxtapose the nuclear peripheral site where spindle pole body (SPB), linker of nucleoskeleton and cytoskeleton (LINC) inserts and participates in accumulating Mis18 complex (70). Such SpCENP-A concentrating factors—for example the LINC component Sad1 (70)—may be a possible candidate to cooperate with Swc2 and Ccp1.

Delocalization of SpCENP-A$^{cnp1\text{-}1}$ from the centromeric chromatin at non-permissive 33°C was previously shown to permit invasion of histone H3 into the centromeric chromatin (29,71), which will need to be evicted to allow reincorporation of SpCENP-A$^{cnp1\text{-}1}$. The chromatin remodeling factors catalyzing histone H3 nucleosome eviction may potentially synergize with Swc2-Ccp1, and one such candidate may be the Ino80 complex, which has been reported to facilitate SpCENP-A incorporation via the removal of histone H3 that has entered into the centromeric chromatin during DNA replication (37,72). Other histone remodeling factor and chaperone candidates that affect SpCENP-A localization, such as the chromo-helicase Chd1-like protein Hrp1 (73,74), may also corroborate with Swc2-Ccp1 in mediating the reincorporation of mislocalized SpCENP-A$^{cnp1\text{-}1}$.

Centromeric DNA is interspersed with sequences that can stall RNAPII and deletion of genes encoding factors that participate in transcription elongation of RNAPII such as Ubp3 or Tfs1 (TFIIS) were reported to facilitate SpCENP-A incorporation into centromeric chromatin, revealing that stalling of RNAPII progression can facilitate implantation of SpCENP-A-nucleosome into centromeric chromatin (34). Similar functional downregulation of transcription elongation factors may also constitute a possible mechanism that synergizes with Swc2 and Ccp1. Future experiments would be required to systematically interrogate all these possibilities.

Besides these SpCENP-A loading factors, our genetic interaction analyses revealed that Set2 collaborates with the canonical SpCENP-A loading factors to reestablish centromeric chromatin after the misincorporated SpCENP-A$^{cnp1\text{-}1}$ is evicted from rDNA and *Δset2* also suppressed mutants of these CENP-A loading factors. Even though *Δset2* could suppress the growth defects of Mis16, Mis17 and Mis18 mutants, *Δset2* could not suppress that of Mis15 and only marginally suppress the Scm3 mutant. While Scm3 is the major CENP-A-binding chaperone that targets SpCENP-A to incorporate into centromeric chromatin (19–22), this weak genetic interaction of *Δset2* with *scm3* may suggest a lower reliance on Scm3, as the SpCENP-A reloading may be co-shouldered by Ccp1, which physically interacts with SpCENP-A, may chaperone SpCENP-A to the Mis16-18 complex (63).

The ability for *Δset2* to revert the mislocalization of WT SpCENP-A in *mis17* mutant at 33°C lends further support to the physiological relevance of Swc2-Ccp1-related mechanism. It is intriguing that *Δset2* can induce SpCENP-A loading in the absence of the Mis17 SpCENP-A loader, pointing to the possible participation of other loading factors that synergize with Mis17 to promote SpCENP-A incorporation. We believe this may entail the collaboration between the SpCENP-A loading facilitators discussed above (e.g. Ino80 complex and SPB components) (70,72) with Mis16-Mis18 complex to confer SpCENP-A incorporation. This is supported by a synergistic genetic interaction of *mis16*, *mis17*, and *mis18* with a gene that encodes Msc1, a SWR1 complex component that physically binds Swc2 (75); suggesting functional redundancy between Mis17 and Mis16–Mis18 complexes. Mutant of the gene encoding Mis6, a key component of Mis17 complex is synthetic lethal with *mis16* mutant further supporting that Mis17 and Mis16-18 complexes function in parallel to complement the function of each other (27). Future research will

be needed to confirm the part played by Swc2–Ccp1 complex in the interaction with the Mis16–Eic1–Mis18 complex, and with different components of the Mis6–Mis15–Mis17–Sim4 complex (25,26), in delineating the factors that synergize with Swc2 and Ccp1 to mediate SpCENP-A relocalization with *Δset2*.

In our study, SpCENP-A$^{cnp1\text{-}1}$ was directed to the rDNA after it delocalized from the centromere. It is currently unclear why rDNA may serve as the preferred sink for delocalized SpCENP-A. Microscopy observation revealed that the clustered centromeres are often situated in the neighborhood of the rDNA locus (76). Due to such positional proximity of the rDNA locus and the centromere in fission yeast, rDNA can function as a 'sink' to trap the misplaced CENP-A before it is dispersed to other parts of the genome to form neocentromeres or aberrant kinetochore structures. Our ChIP analysis did not detect mislocalized SpCENP-A$^{cnp1\text{-}1}$ at previously reported neocentromere sites (49), which may due to the presence of mechanisms that prevent such CENP-A incorporation, such as the presence of histone H2A.Z, which counteracts CENP-A incorporation at these sites (49). This and other mechanisms may cause the formation of a neocentromere to be stochastic and requires a longer period of time to establish after the endogenous centromere is inactivated (8,48,49).

In contrast, SpCENP-A$^{cnp1\text{-}1}$ was detected on the rDNA locus within one cell cycle; this suggests that the delocalization of a large amount of SpCENP-A from the centromere triggers a back-up pathway to restore CENP-A localization. Such relocalization would thus require Ccp1 and Swc2 to also be targeted to rDNA, which we have detected. Because Ccp1 localization is dependent on SpCENP-A, the concentration of delocalized SpCENP-A$^{cnp1\text{-}1}$ at rDNA under restrictive conditions may aid in directing Ccp1 to rDNA. Alternatively, many rDNA localizing factors (for example, Gar1 and Gar2) can also bind Ccp1 and contribute to attracting Ccp1 to rDNA repeats (64). Subsequent remodeling of the chromatin at the rDNA locus by the SWR1 complex may further stabilize Ccp1 recruitment, since the latter was reported to bind histone H2A.Z chaperoned by SWR1 (61,63).

Set2 is often associated with transcriptional elongation (77,78). Our work herein thus uncovered a novel role of Set2 in stabilizing Ccp1 at the fission yeast centromere. Ccp1 is involved in ensuring proper localization of centromeric factors, including Mis6 and Sim4, and prevents invasion by flanking heterochromatin (64). Hence, although Ccp1 is reported as a CENP-A disassembly factor (63), this activity appears to only occur at extra-centromeric loci, including rDNA sequences in the nucleolus, but not at centromeres (63,64). It is intriguing to consider what might control the outcomes of Ccp1-disassembly activities at different loci, and it is tempting to speculate that Ccp1 activity might be differentially modulated by its binding partners: binding to Set2 at the centromere might repress its action, whereas its association with factors such as Swc2 at the rDNA may result in activating the disassembly activity of Ccp1.

What then may be the relationship of H3K36 methylation in the Set2-Swc2-Ccp1-linked relocalization of SpCENP-A? The results of different experiments performed in *Δset2*, Set2 SET domain mutant *set2-D295AY296A* and *H3K36R* seemed not entirely in agreement with one another pointing to a differential involvement of Set2 protein, its catalytic activity and its most well-known target, H3K36 in this mechanism. The spotting assay visualizing the degree of suppression of *cnp1-1* temperature sensitive growth defect was the only experiment that showed agreement between these three components. The results of the other tests—ChIP of SpCENP-A$^{cnp1\text{-}1}$ and increase in *swc2*$^{+}$ expression—showed consistency between *Δset2* and *set2-D295AY296A*, but not with *H3K36R*, which actually resembled WT. Even though more similar to WT, *H3K36R* did yield an intermediate outcome in the re-formation of centromeric spot localization of SpCENP-A$^{cnp1\text{-}1}$ under fluorescent microscopy. These results point to the requirement of Set2 protein, its catalytic activity and H3K36 target in safeguarding the viability of *cnp1-1*, which entails the accumulation of SpCENP-A$^{cnp1\text{-}1}$ at the centromeric vicinity and the subsequent incorporation into the centromeric chromatin, as detailed above. While the microscopic centromeric spots scored for the signals of both SpCENP-A$^{cnp1\text{-}1}$ residing in centromeric vicinity and within chromatin, ChIP delineates the SpCENP-A$^{cnp1\text{-}1}$ chromatin-incorporated population. Thus it appeared that H3K36 is needed for *cnp1-1* survival, possibly participating in concentration of SpCENP-A$^{cnp1\text{-}1}$ in the nuclear compartment surrounding centromere, which functions distinctly from the Swc2-dependent regulation (Supplementary Figure S16). The requirement of Set2 and its catalytic activity (but not H3K36) for the Swc2-Ccp1-mechanism suggest that there may be methylation targets other than H3K36, and a possibility maybe transcription repressors of the *swc2*$^{+}$ transcription.

Furthermore, the intriguing suppression of growth and chromosome segregation defects by H3K36R without similar level of SpCENP-A$^{cnp1\text{-}1}$ centromere relocalization as that of *Δset2* suggest that disruption of H3K36 may somehow reduce the requirement of SpCENP-A on the centromeres for kinetochore assembly and/or faithful chromosome segregation. This possibility could potentially be achieved via enhancing the activity of pathways that function in parallel to that of SpCENP-A and one of such may involves Mis12 (12,27,79,80). Mis12 constitutes part of the complex that mount the adaptor Ndc80 complex to stabilize kinetochore microtubule for orchestrating precise chromosome segregation during M-phase. This in turn is suggestive of a function in the restriction of kinetochore-microtubule attachment activity by Set2 via H3K36 methylation. If so, the concomitant modulation of microtubule attachment and promotion of SpCENP-A relocalization via Swc2-Ccp1 might then simultaneously cooperate to rescue *cnp1-1* defects by depletion of *set2* (Supplementary Figure S16).

In conclusion, our work identified a novel pathway involving two chromatin remodelers—Swc2 and Ccp1—in conjunction with Set2 to function in a feedback regulation to redirect delocalized SpCENP-A back to the centromere via evicting mis-incorporated SpCENP-A from rDNA locus. Chromosome missegregation is a severe genetic instability event that compromises cell viability (12,81,82). This mechanism thus promotes CENP-A presence at the centromere to maintain genomic stability.

Data availability

The RNA sequencing data underlying this article is available in Gene Expression Omnibus at https://www.ncbi.nlm.nih.gov/geo/, under the accession code of GSE196504.

Supplementary data

Supplementary Data are available at NAR Online.

Acknowledgements

We thank R. Jackson for critically editing the manuscript, R. Raechell for technical support, K. Gull for αTAT1 antibody, M. Yanagida, Y. Hiraoka and National BioResource Project (NBRP) (Japan) for yeast strains.

Funding

Tier 2 Academic Research Grants from Singapore Ministry of Education [MOE2016-T2-2-063, MOE2018-T2-1-100, NUHSRO/2023/043/T1/Seed-Mar/03]; National University Health System [NUHSRO/2021/062/NUSMed/04/LOA] awarded to E.S.C. Funding for open access charge: Ministry of Education, Singapore.

Conflict of interest statement

None declared.

References

1. Ganmore,I., Smooha,G. and Izraeli,S. (2009) Constitutional aneuploidy and cancer predisposition. *Hum. Mol. Genet.*, **18**, R84–R93.
2. Jackson,R.A., Nguyen,M.L., Barrett,A.N., Tan,Y.Y., Choolani,M.A. and Chen,E.S. (2016) Synthetic combinations of missense polymorphic genetic changes underlying Down syndrome susceptibility. *Cell. Mol. Life Sci.*, **73**, 4001–4017.
3. Hanahan,D. and Weinberg,R.A. (2011) Hallmarks of cancer: the next generation. *Cell*, **144**, 646–674.
4. Pfau,S.J. and Amon,A. (2012) Chromosomal instability and aneuploidy in cancer: from yeast to man. *EMBO Rep.*, **13**, 515–527.
5. Musacchio,A. and Desai,A. (2017) A molecular view of kinetochore assembly and function. *Biology (Basel)*, **6**, 5.
6. Allshire,R.C. and Karpen,G.H. (2008) Epigenetic regulation of centromeric chromatin: old dogs, new tricks?*Nat. Rev. Genet.*, **9**, 923–937.
7. Westhorpe,F.G. and Straight,A.F. (2014) The centromere: epigenetic control of chromosome segregation during mitosis. *Cold Spring Harb. Perspect. Biol.*, **7**, a015818.
8. DeBose-Scarlett,E.M. and Sullivan,B.A. (2021) Genomic and epigenetic foundations of neocentromere formation. *Annu. Rev. Genet.*, **55**, 331–348.
9. Guse,A., Carroll,C.W., Moree,B., Fuller,C.J. and Straight,A.F. (2011) In vitro centromere and kinetochore assembly on defined chromatin templates. *Nature*, **477**, 354–358.
10. Mendiburo,M.J., Padeken,J., Fulop,S., Schepers,A. and Heun,P. (2011) Drosophila CENH3 is sufficient for centromere formation. *Science*, **334**, 686–690.
11. Sekulic,N. and Black,B.E. (2012) Molecular underpinnings of centromere identity and maintenance. *Trends Biochem. Sci.*, **37**, 220–229.
12. Takahashi,K., Chen,E.S. and Yanagida,M. (2000) Requirement of Mis6 centromere connector for localizing a CENP-A-like protein in fission yeast. *Science*, **288**, 2215–2219.
13. Tomonaga,T., Matsushita,K., Yamaguchi,S., Oohashi,T., Shimada,H., Ochiai,T., Yoda,K. and Nomura,F. (2003) Overexpression and mistargeting of centromere protein-A in human primary colorectal cancer. *Cancer Res.*, **63**, 3511–3516.
14. Shrestha,R.L., Ahn,G.S., Staples,M.I., Sathyan,K.M., Karpova,T.S., Foltz,D.R. and Basrai,M.A. (2017) Mislocalization of centromeric histone H3 variant CENP-A contributes to chromosomal instability (CIN) in human cells. *Oncotarget*, **18**, 46781–46800
15. Qiu,J.J., Guo,J.J., Lv,T.J., Jin,H.Y., Ding,J.X., Feng,W.W., Zhang,Y. and Hua,K.Q. (2013) Prognostic value of centromere protein-A expression in patients with epithelial ovarian cancer. *Tumour Biol.*, **34**, 2971–2975.
16. Wu,Q., Qian,Y.M., Zhao,X.L., Wang,S.M., Feng,X.J., Chen,X.F. and Zhang,S.H. (2012) Expression and prognostic significance of centromere protein A in human lung adenocarcinoma. *Lung. Cancer*, **77**, 407–414.
17. McGovern,S.L., Qi,Y., Pusztai,L., Symmans,W.F. and Buchholz,T.A. (2012) Centromere protein-A, an essential centromere protein, is a prognostic marker for relapse in estrogen receptor-positive breast cancer. *Breast Cancer Res.*, **14**, R72.
18. Li,Y., Zhu,Z., Zhang,S., Yu,D., Yu,H., Liu,L., Cao,X., Wang,L., Gao,H. and Zhu,M. (2011) ShRNA-targeted centromere protein A inhibits hepatocellular carcinoma growth. *PLoS One*, **6**, e17794.
19. Williams,J.S., Hayashi,T., Yanagida,M. and Russell,P. (2009) Fission yeast Scm3 mediates stable assembly of Cnp1/CENP-A into centromeric chromatin. *Mol. Cell*, **33**, 287–298.
20. Pidoux,A.L., Choi,E.S., Abbott,J.K., Liu,X., Kagansky,A., Castillo,A.G., Hamilton,G.L., Richardson,W., Rappsilber,J., He,X., *et al.* (2009) Fission yeast Scm3: a CENP-A receptor required for integrity of subkinetochore chromatin. *Mol. Cell*, **13**, 299–311.
21. Dunleavy,E.M., Roche,D., Tagami,H., Lacoste,N., Ray-Gallet,D., Nakamura,Y., Daigo,Y., Nakatani,Y. and Almouzni-Pettinotti,G. (2009) HJURP is a cell-cycle-dependent maintenance and deposition factor of CENP-A at centromeres. *Cell*, **1**, 485–497.
22. Foltz,D.R., Jansen,L.E., Bailey,A.O., Yates,J.R.3r., Bassett,E.A., Wood,S., Black,B.E. and Cleveland,D.W. (2009) Centromere-specific assembly of CENP-a nucleosomes is mediated by HJURP. *Cell*, **1**, 472–484.
23. Dunleavy,E.M., Pidoux,A.L., Monet,M., Bonilla,C., Richardson,W., Hamilton,G.L., Ekwall,K., McLaughlin,P.J. and Allshire,R.C. (2007) A NASP (N1/N2)-related protein, Sim3, binds CENP-A and is required for its deposition at fission yeast centromeres. *Mol. Cell*, **28**, 1029–1044.
24. Tan,H.L., Lim,K.K., Yang,Q., Fan,J.S., Sayed,A.M.M., Low,L.S., Ren,B., Lim,T.K., Lin,Q., Mok,Y.K., *et al.* (2018) Prolyl isomerization of the CENP-A N-terminus regulates centromeric integrity in fission yeast. *Nucleic Acids Res.*, **46**, 1167–1179.
25. Shiroiwa,Y., Hayashi,T., Fujita,Y., Villar-Briones,A., Ikai,N., Takeda,K., Ebe,M. and Yanagida,M. (2011) Mis17 is a regulatory module of the Mis6-Mal2-Sim4 centromere complex that is required for the recruitment of CenH3/CENP-A in fission yeast. *PLoS One*, **21**, e17761.
26. Xu,X., Nakazawa,N., Wang,L., Arakawa,O. and Yanagida,M. (2019) Negative regulation of the Mis17-Mis6 centromere complex by mRNA decay pathway and EKC/KEOPS complex in Schizosaccharomyces pombe. *G3*, **9**, 1815–1823.
27. Hayashi,T., Fujita,Y., Iwasaki,O., Adachi,Y., Takahashi,K. and Yanagida,M. (2004) Mis16 and Mis18 are required for CENP-A loading and histone deacetylation at centromeres. *Cell*, **118**, 715–729.
28. Hori,T., Amano,M., Suzuki,A., Backer,C.B., Welburn,J.P., Dong,Y., McEwen,B.F., Shang,W.H., Suzuki,E., Okawa,K., *et al.* (2008) CCAN makes multiple contacts with centromeric DNA to provide distinct pathways to the outer kinetochore. *Cell*, **135**, 1039–1052.
29. Chen,E.S., Saitoh,S., Yanagida,M. and Takahashi,K. (2003) A cell cycle-regulated GATA factor promotes centromeric localization of CENP-A in fission yeast. *Mol. Cell*, **11**, 175–187.
30. Takayama,Y., Sato,H., Saitoh,S., Ogiyama,Y., Masuda,F. and Takahashi,K. (2008) Biphasic incorporation of centromeric histone CENP-A in fission yeast. *Mol. Biol. Cell*, **19**, 682–690.
31. Takahashi,K., Takayama,Y., Masuda,F., Kobayashi,Y. and Saitoh,S. (2005) Two distinct pathways responsible for the loading of CENP-A to centromeres in the fission yeast cell cycle. *Philos. Trans. R. Soc. Lond. B Biol. Sci.*, **360**, 595–606.
32. Quenet,D. and Dalal,Y. (2014) A long non-coding RNA is required for targeting centromeric protein A to the human centromere. *eLife*, **3**, e03254.
33. Bobkov,G.O.M., Gilbert,N. and Heun,P. (2018) Centromere transcription allows CENP-A to transit from chromatin association to stable incorporation. *J. Cell Biol.*, **217**, 1957–1972.

34. Catania,S., Pidoux,A.L. and Allshire,R.C. (2015) Sequence features and transcriptional stalling within centromere DNA promote establishment of CENP-A chromatin. *PLoS Genet.*, **11**, e1004986.
35. Bobkov,G.O.M., Huang,A., van den Berg,S.J.W., Mitra,S., Anselm,E., Lazou,V., Schunter,S., Feederle,R., Imhof,A., Lusser,A., *et al.* (2020) Spt6 is a maintenance factor for centromeric CENP-A. *Nat. Commun.*, **11**, 2919.
36. Dunleavy,E.M., Almouzni,G. and Karpen,G.H. (2011) H3.3 is deposited at centromeres in S phase as a placeholder for newly assembled CENP-A in G1 phase. *Nucleus*, **2**, 146–157.
37. Shukla,M., Tong,P., White,S.A., Singh,P.P., Reid,A.M., Catania,S., Pidoux,A.L. and Allshire,R.C. (2018) Centromere DNA Destabilizes H3 Nucleosomes to Promote CENP-A Deposition during the Cell Cycle. *Curr. Biol.*, **28**, 3924–3936.
38. Zhu,J., Cheng,K.C.L. and Yuen,K.W.Y. (2018) Histone H3K9 and H4 acetylations and transcription facilitate the initial CENP-A^{HCP-3} deposition and de novo centromere establishment in Caenorhabditis elegans artificial chromosomes. *Epigenetics Chromatin*,**11**, 16.
39. Lim,K.K., Ong,T.Y., Tan,Y.R., Yang,E.G., Ren,B., Seah,K.S., Yang,Z., Tan,T.S., Dymock,B.W. and Chen,E.S. (2015) Mutation of histone H3 serine 86 disrupts GATA factor Ams2 expression and precise chromosome segregation in fission yeast. *Sci. Rep.*, **5**, 14064.
40. Nguyen,T.T., Lim,J.S., Tang,R.M., Zhang,L. and Chen,E.S. (2015) Fitness profiling links topoisomerase II regulation of centromeric integrity to doxorubicin resistance in fission yeast. *Sci. Rep.*, **5**, 8400.
41. Tan,H.L. and Chen,E.S. (2022) GRANT motif regulates CENP-A incorporation and restricts RNA polymerase II accessibility at centromere. *Genes (Basel)*, **13**, 1697.
42. Nakabayashi,Y. and Seki,M. (2022) Transcription destabilizes centromere function. *Biochem. Biophys. Res. Commun.*, **586**, 150–156.
43. Collins,K.A., Furuyama,S. and Biggins,S. (2004) Proteolysis contributes to the exclusive centromere localization of the yeast Cse4/CENP-A histone H3 variant. *Curr. Biol.*, **14**, 1968–1972.
44. Moreno-Moreno,O., Torras-Llort,M. and Azorín,F. (2006) Proteolysis restricts localization of CID, the centromere-specific histone H3 variant of Drosophila, to centromeres. *Nucleic Acids Res.*,**34**, 6247–6255.
45. Au,W.C., Zhang,T., Mishra,P.K., Eisenstatt,J.R., Walker,R.L., Ocampo,J., Dawson,A., Warren,J., Costanzo,M., Baryshnikova,A., *et al.* (2020) Skp, Cullin, F-box (SCF)-Met30 and SCF-Cdc4-mediated proteolysis of CENP-A prevents mislocalization of CENP-A for chromosomal stability in budding yeast. *PLoS Genet.*, **16**, e1008597.
46. Wang,K., Liu,Y., Yu,Z., Gu,B., Hu,J., Huang,L., Ge,X., Xu,L., Zhang,M., Zhao,J., *et al.* (2021) Phosphorylation at Ser68 facilitates DCAF11-mediated ubiquitination and degradation of CENP-A during the cell cycle. *Cell Rep.*, **37**, 109987.
47. Shrestha,R.L., Rossi,A., Wangsa,D., Hogan,A.K., Zaldana,K.S., Suva,E., Chung,Y.J., Sanders,C.L., Difilippantonio,S., Karpova,T.S., *et al.* (2021) CENP-A overexpression promotes aneuploidy with karyotypic heterogeneity. *J. Cell Biol.*, **220**, e202007195.
48. Ishii,K., Ogiyama,Y., Chikashige,Y., Soejima,S., Masuda,F., Kakuma,T., Hiraoka,Y. and Takahashi,K. (2008) Heterochromatin integrity affects chromosome reorganization after centromere dysfunction. *Science*, **321**, 1088–1091.
49. Ogiyama,Y., Ohno,Y., Kubota,Y. and Ishii,K. (2013) Epigenetically induced paucity of histone H2A.Z stabilizes fission-yeast ectopic centromeres. *Nat. Struct. Mol. Biol.*, **20**, 1397–1406.
50. Forsburg,S.L. and Rhind,N. (2006) Basic methods for fission yeast. *Yeast*, **23**, 173–183.
51. Moreno,S., Klar,A. and Nurse,P. (1991) Molecular genetic analysis of fission yeast Schizosaccharomyces pombe. *Methods Enzymol.*, **194**, 795–823.
52. Lim,K.K., Nguyen,T.T.T., Li,A.Y., Yeo,Y.P. and Chen,E.S. (2018) Histone H3 lysine 36 methyltransferase mobilizes NER factors to regulate tolerance against alkylation damage in fission yeast. *Nucleic Acids Res.*, **46**, 5061–5074.
53. Lim,K.K. and Chen,E.S. (2018) Systematic quantification of GFP-tagged protein foci in Schizosaccharomyces pombe nuclei. *Bio Protoc.*, **8**, e3117.
54. Ren,B., Tan,H.L., Nguyen,T.T.T., Sayed,A.M.M., Li,Y., Mok,Y.K., Yang,H. and Chen,E.S. (2018) Regulation of transcriptional silencing and chromodomain protein localization at centromeric heterochromatin by histone H3 tyrosine 41 phosphorylation in fission yeast. *Nucleic Acids Res.*, **46**, 189–202.
55. Anders,S., Pyl,P.T. and Huber,W. (2015) HTSeq—a Python framework to work with high-throughput sequencing data. *Bioinformatics*, **31**, 166–169.
56. Woods,A., Sherwin,T., Sasse,R., MacRae,T.H., Baines,A.J. and Gull,K. (1989) Definition of individual components within the cytoskeleton of Trypanosoma brucei by a library of monoclonal antibodies. *J. Cell Sci.*, **93**, 491–500.
57. Morris,S.A., Shibata,Y., Noma,K., Tsukamoto,Y., Warren,E., Temple,B., Grewal,S.I. and Strahl,B.D. (2005) Histone H3 K36 methylation is associated with transcription elongation in Schizosaccharomyces pombe. *Euk. Cell*, **4**, 1446–1454.
58. Chen,C.C., Bowers,S., Lipinszki,Z., Palladino,J., Trusiak,S., Bettini,E., Rosin,L., Przewloka,M.R., Glover,D.M., O'Neill,R.J., *et al.* (2015) Establishment of centromeric chromatin by the CENP-A assembly factor CAL1 requires FACT-mediated transcription. *Dev. Cell*, **34**, 73–84.
59. McDaniel,S.L. and Strahl,B.D. (2017) Shaping the cellular landscape with Set2/SETD2 methylation. *Cell. Mol. Life Sci.*, **74**, 3317–3334.
60. Basi,G., Schmid,E. and Maundrell,K. (1993) TATA box mutations in the Schizosaccharomyces pombe nmt1 promoter affect transcription efficiency but not the transcription start point or thiamine repressibility. *Gene*, **123**, 131–136.
61. Yen,K., Vinayachandran,V. and Pugh,B.F. (2013) SWR-C and INO80 chromatin remodelers recognize nucleosome-free regions near +1 nucleosomes. *Cell*, **154**, 1246–1256.
62. Maundrell,K. (1990) nmt1 of fission yeast. A highly transcribed gene completely repressed by thiamine. *J. Biol. Chem.*, **265**, 10857–10864.
63. Dong,Q., Yin,F.X., Gao,F., Shen,Y., Zhang,F., Li,Y., He,H., Gonzalez,M., Yang,J., Zhang,S., *et al.* (2016) Ccp1 homodimer mediates chromatin integrity by antagonizing CENP-A loading. *Mol. Cell*, **64**, 79–91.
64. Lu,M. and He,X. (2018) Ccp1 modulates epigenetic stability at centromeres and affects heterochromatin distribution in Schizosaccharomyces pombe. *J. Biol. Chem.*, **293**, 12068–12080.
65. Dronamraju,R., Jha,D.K., Eser,U., Adams,A.T., Dominguez,D., Choudhury,R., Chiang,Y.C., Rathmell,W.K., Emanuele,M.J., Churchman,L.S., *et al.* (2018) Set2 methyltransferase facilitates cell cycle progression by maintaining transcriptional fidelity. *Nucleic Acids Res.*, **46**, 1331–1344.
66. Bhattacharya,S., Lange,J.J., Levy,M., Florens,L., Washburn,M.P. and Workman,J.L. (2021) The disordered regions of the methyltransferase SETD2 govern its function by regulating its proteolysis and phase separation. *J. Biol. Chem.*, **297**, 101075.
67. Takeda,K., Mori,A. and Yanagida,M. (2011) Identification of genes affecting the toxicity of anti-cancer drug bortezomib by genome-wide screening in S. pombe. *PLoS One*, **6**, e22021.
68. Bade,D., Pauleau,A.L., Wendler,A. and Erhardt,S. (2014) The E3 ligase CUL3/RDX controls centromere maintenance by ubiquitylating and stabilizing CENP-A in a CAL1-dependent manner. *Dev. Cell*, **28**, 508–519.
69. Ohkuni,K., Gliford,L., Au,W.C., Suva,E., Kaiser,P. and Basrai,M.A. (2022) Cdc48Ufd1/Npl4 segregase removes mislocalized centromeric histone H3 variant CENP-A from non-centromeric chromatin. *Nucleic Acids Res.*, **50**, 3276–3291.
70. London,N., Medina-Pritchard,B., Spanos,C., Rappsilber,J., Jeyaprakash,A.A. and Allshire,R.C. (2023) Direct recruitment of

Mis18 to interphase spindle pole bodies promotes CENP-A chromatin assembly. *Curr. Biol.*, **33**, 4187–4201.
71. Chen,E.S., Yanagida,M. and Takahashi,K. (2003) Does a GATA factor make the bed for centromeric nucleosomes. *Cell Cycle*, **2**, 277–278.
72. Singh,P.P., Shukla,M., White,S.A., Lafos,M., Tong,P., Auchynnikava,T., Spanos,C., Rappsilber,J., Pidoux,A.L. and Allshire,R.C. (2020) Hap2-Ino80-facilitated transcription promotes de novo establishment of CENP-A chromatin. *Genes Dev.*, **34**, 226–238.
73. Walfridsson,J., Bjerling,P., Thalen,M., Yoo,E.J., Park,S.D. and Ekwall,K. (2005) The CHD remodeling factor Hrp1 stimulates CENP-A loading to centromeres. *Nucleic Acids Res.*, **33**, 2868–2879.
74. Choi,E.S., Strålfors,A., Castillo,A.G., Durand-Dubief,M., Ekwall,K. and Allshire,R.C. (2011) Identification of noncoding transcripts from within CENP-A chromatin at fission yeast centromeres. *J. Biol. Chem.*, **286**, 23600–23607.
75. Hou,H., Wang,Y., Kallgren,S.P., Thompson,J., Yates,J.R. and Jia,S. (2010) Histone variant H2A.Z regulates centromere silencing and chromosome segregation in fission yeast. *J. Biol. Chem.*, **285**, 1909–1918.
76. Uzawa,S. and Yanagida,M. (1992) Visualization of centromeric and nucleolar DNA in fission yeast by fluorescence in situ hybridization. *J. Cell Sci.*, **101**, 267–275.
77. Huang,C. and Zhu,B. (2018) Roles of H3K36-specific histone methyltransferases in transcription: antagonizing silencing and safeguarding transcription fidelity. *Biophys. Rep.*, **4**, 170–177.
78. Lam,U.T.F. and Chen,E.S. (2022) Molecular mechanisms in governing genomic stability and tumor suppression by the SETD2 H3K36 methyltransferase. *Int. J. Biochem. Cell Biol.*, **144**, 106155.
79. Obuse,C., Iwasaki,O., Kiyomitsu,T., Goshima,G., Toyoda,Y. and Yanagida,M. (2004) A conserved Mis12 centromere complex is linked to heterochromatic HP1 and outer kinetochore protein Zwint-1. *Nat. Cell Biol.*, **6**, 1135–1141.
80. Goshima,G., Kiyomitsu,T., Yoda,K. and,Y. M. (2003) Human centromere chromatin protein hMis12, essential for equal segregation, is independent of CENP-A loading pathway. *J. Cell Biol.*, **160**, 25–39.
81. Eyre-Walker,A. and Keightley,P.D. (2007) The distribution of fitness effects of new mutations. *Nat. Rev. Genet.*, **8**, 610–618.
82. Gug,C., Ratiu,A., Navolan,D., Dragan,I., Groza,I.M., Papurica,M., Vaida,M.A., Mozos,I. and Jurca,M.C. (2019) Incidence and spectrum of chromosome abnormalities in miscarriage samples: a retrospective study of 330 cases. *Cytogenet. Genome Res.*, **158**, 171–183.

Received: May 2, 2023. **Revised:** January 24, 2024. **Editorial Decision:** January 24, 2024. **Accepted:** January 29, 2024